Cell Reports

Article

Nogo-B inhibition facilitates cholesterol metabolism to reduce hypercholesterolemia

Graphical abstract

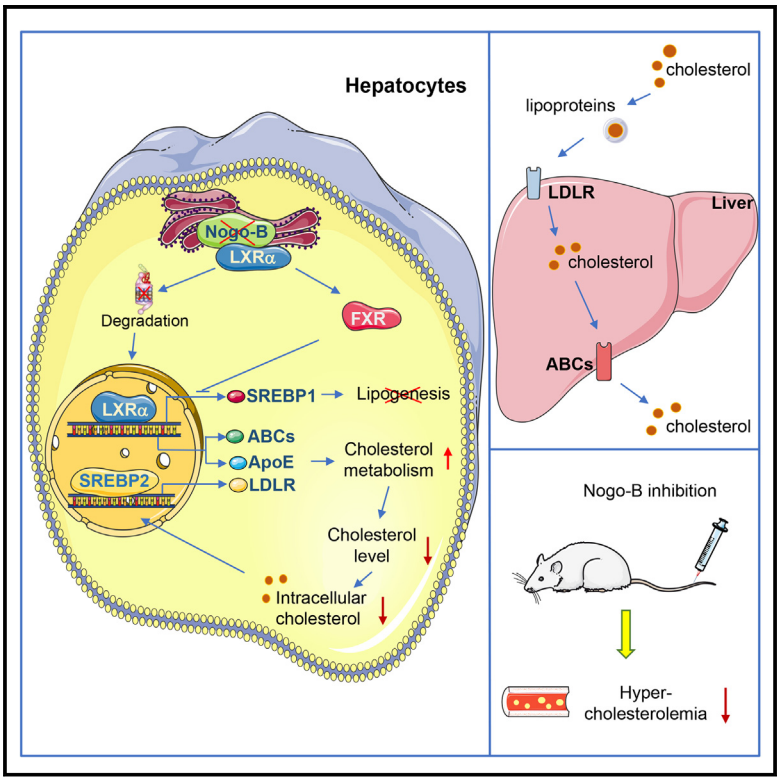

Highlights

- Interaction between Nogo-B and LXRα increases LXRα-ubiquitinated degradation
- Nogo-B deficiency inhibits the LXRα-SREBP1 axis by activating FXR expression
- Nogo-B inhibition effectively reduces hypercholesterolemia
- Nogo-B inhibition promotes liver uptake for cholesterol and cholesterol excretion

Authors

Chao Xue, Peng Zeng, Ke Gong, ..., Yuanli Chen, Houzao Chen, Yajun Duan

Correspondence

chenyuanli@hfut.edu.cn (Y.C.), chenhouzao@ibms.cams.cn (H.C.), yajunduan@ustc.edu.cn (Y.D.)

In brief

Xue et al. present a mechanism for the regulation of cholesterol metabolism. Nogo-B deficiency not only promotes cholesterol excretion by increasing LXR stability but also enhances hepatic uptake for cholesterol.

Xue et al., 2024, Cell Reports *43*, 114691
September 24, 2024
https://doi.org/10.1016/j.celrep.2024.114691

CellPress

Cell Reports

CellPress
OPEN ACCESS

Article

Nogo-B inhibition facilitates cholesterol metabolism to reduce hypercholesterolemia

Chao Xue,[1,2] Peng Zeng,[2] Ke Gong,[3] Qian Li,[2] Zian Feng,[1] Mengyao Wang,[3] Shasha Chen,[3] Yanfang Yang,[2] Jiaqi Li,[2] Shuang Zhang,[3] Zequn Yin,[1] Yingquan Liang,[3] Tengteng Yan,[3] Miao Yu,[4] Ke Feng,[2] Dan Zhao,[2] Xiaoxiao Yang,[3] Xia Zhang,[5] Likun Ma,[1] Yasuko Iwakiri,[6] Liang Chen,[7] Xiaoqiang Tang,[8] Yuanli Chen,[3,*] Houzao Chen,[9,*] and Yajun Duan[1,10,*]

[1]Department of Cardiology, the First Affiliated Hospital of USTC, Division of Life Sciences and Medicine, University of Science and Technology of China, Hefei, Anhui 230001, China

[2]College of Life Sciences, Key Laboratory of Bioactive Materials of Ministry of Education, State Key Laboratory of Medicinal Chemical Biology, Nankai University, Tianjin 300071, China

[3]Key Laboratory of Metabolism and Regulation for Major Diseases of Anhui Higher Education Institutes, College of Food and Biological Engineering, Hefei University of Technology, Hefei 230009, China

[4]Medical College of Soochow University, Suzhou 215031, China

[5]Tianjin Baodi Hospital, Baodi Clinical College of Tianjin Medical University, Tianjin 301800, China

[6]Section of Digestive Diseases, Yale University School of Medicine, New Haven, CT 06519, USA

[7]College of Life Science, Anhui Medical University, Hefei 230032, China

[8]Key Laboratory of Birth Defects and Related Diseases of Women and Children of MOE, State Key Laboratory of Biotherapy, West China Second University Hospital, Sichuan University, No. 17 People's South Road, Chengdu, Sichuan 610041, China

[9]Department of Biochemistry & Molecular Biology, State Key Laboratory of Common Mechanism Research for Major Diseases, Institute of Basic Medical Sciences, Chinese Academy of Medical Sciences & Peking Union Medical College, 5 Dong Dan San Tiao, Beijing 100005, China

[10]Lead contact

*Correspondence: chenyuanli@hfut.edu.cn (Y.C.), chenhouzao@ibms.cams.cn (H.C.), yajunduan@ustc.edu.cn (Y.D.)

https://doi.org/10.1016/j.celrep.2024.114691

SUMMARY

The strategy of lowering cholesterol levels by promoting cholesterol excretion is still lacking, and few molecular targets act on multiple cholesterol metabolic processes. In this study, we find that Nogo-B deficiency/inhibition simultaneously promotes hepatic uptake of cholesterol and cholesterol excretion. Nogo-B deficiency decreases cholesterol levels by activating ATP-binding cassette transporters (ABCs), apolipoprotein E (ApoE), and low-density lipoprotein receptor (LDLR) expression. We discover that Nogo-B interacts with liver X receptor α (LXRα), and Nogo-B deficiency inhibits ubiquitination degradation of LXRα, thereby enhancing its function on cholesterol excretion. Decreased cellular cholesterol levels further activate SREBP2 and LDLR expression, thereby promoting hepatic uptake of cholesterol. Nogo-B inhibition decreases atherosclerotic plaques and cholesterol levels in mice, and Nogo-B levels are correlated to cholesterol levels in human plasma. In this study, Nogo-B deficiency/inhibition not only promotes hepatic uptake of blood cholesterol but also facilitates cholesterol excretion. This study reports a strategy to lower cholesterol levels by inhibiting Nogo-B expression to promote hepatic cholesterol uptake and cholesterol excretion.

INTRODUCTION

Hypercholesterolemia, which is characterized by high cholesterol levels in the serum, is a major risk factor for metabolic syndrome and coronary artery diseases such as atherosclerosis and heart attacks.[1] Analysis of the Framingham Heart Study and Kaiser Permanente Heart Study has shown that cholesterol levels are significantly associated with the risk of cardiovascular mortality.[2] In particular, low-density lipoprotein-cholesterol (LDL-C) is strongly proportional to the occurrence of atherosclerotic cardiovascular disease (ASCVD), and reducing the level of LDL-C has been closely linked to reducing cardiovascular mortality in patients with higher baseline levels of LDL-C (>100 mg/dL).[3,4]

Hypercholesterolemia can be directly caused by abnormalities in cholesterol metabolism. Liver is the main site for cholesterol metabolism. Lipoproteins rich in cholesterol esters, encapsulated with apolipoprotein B (ApoB) and ApoE, are recognized by LDL receptors (LDLR) and absorbed into the liver.[5] Liver cholesterol can be metabolized into bile acids or excreted into peripheral tissues through ATP-binding cassette transporters (ABCs) and eventually excreted into the feces.[6] Hepatic cholesterol is excreted into the bile duct and intestinal lumen through ABCG5/ABCG8.[6] Cholesterol can also be excreted into peripheral tissues through ABCA1.[7] Abnormal cholesterol metabolism in the liver directly destroys the homeostasis of cholesterol levels in the liver and blood, which may induce nonalcoholic fatty liver

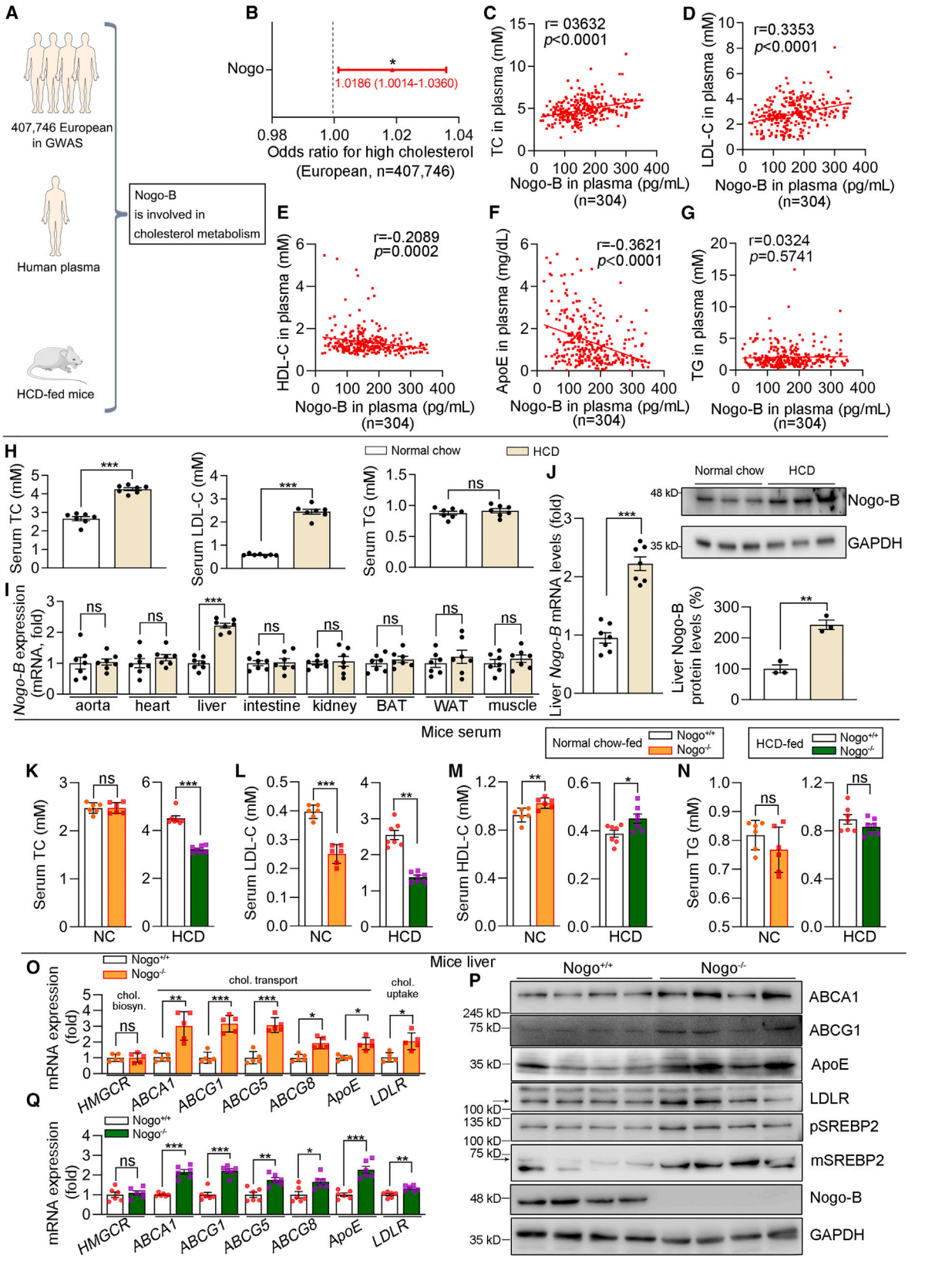

(legend on next page)

disease, nonalcoholic steatohepatitis, and ASCVD.[8] However, the regulatory mechanisms of cholesterol metabolism remain to be elucidated. The current methods of reducing hypercholesterolemia are mainly to intervene in the cholesterol metabolism process. The cholesterol-lowering drugs, including statins and PCSK9 inhibitors, are first-line drugs for patients with hypercholesterolemia and ASCVD.[9] Statins, the inhibitors of cholesterol synthesis rate-limiting enzyme 3-hydroxy-3-methylglutaryl coenzyme A reductase (HMGCR), reduces serum cholesterol levels by inhibiting cholesterol biosynthesis and promoting LDL-C uptake by activating LDLR expression. PCSK9 inhibitors decrease the degradation of LDLR, thereby promoting the uptake of circulating LDL-C. Notably, there are no existing cholesterol-lowering drugs targeting the process of cholesterol excretion, and few molecular targets act on multiple cholesterol metabolic processes.

Nogo-B has attracted our attention because of its role in metabolic processes. The Nogo (Reticulon 4) family is located in the endoplasmic reticulum and consists of several members, including Nogo-A, Nogo-B and Nogo-C, with an alternatively spliced transcript variant.[10] Nogo-A and Nogo-C are expressed mainly in the CNS, while Nogo-B is expressed in multiple tissues.[11] Nogo-B is also the only Nogo member detectable in the circulation and liver.[12] We have found that Nogo-B is involved in multiple metabolic processes and diseases, such as high-carbohydrate diet-induced liver steatosis,[12] white adipogenesis,[13] and obesity.[14] For instance, our previous study found that Nogo-B deficiency reduced high-glucose or high-fructose diet-induced hepatic steatosis by decreasing carbohydrate response element binding protein-mediated lipogenesis.[12] Many studies have found that Nogo-B is involved in triglyceride (TG) metabolism[12,14,15]; however, few studies have focused on the role of Nogo-B in cholesterol metabolism and related metabolic diseases.

In this study, we identified an unrecognized role of Nogo-B in cholesterol metabolism by mediating hepatic uptake of cholesterol and cholesterol excretion. Nogo-B deficiency decreased cholesterol levels by promoting cholesterol excretion and reducing hepatocyte cholesterol levels, thereby promoting the liver uptake of cholesterol by activating SREBP2 and LDLR expression. Plasma Nogo-B exhibited tight correlation with cholesterol levels in humans. Nogo-B deficiency decreased cholesterol levels in high-cholesterol diet (HCD)-fed mice, and Nogo-B inhibition alleviated hypercholesterolemia and ASCVD. Interestingly, our previous study found that Nogo-B deficiency reduced TG levels under high-fat diet (HFD) feeding[14]; however, we found that Nogo-B did not affect TG levels under HCD feeding, which should be attributed to the regulation of liver X receptor α (LXRα). Here, Nogo-B deficiency/inhibition not only promotes hepatic uptake of cholesterol by activating LDLR expression but it also promotes cholesterol excretion by enhancing LXRα expression, which provides a strategy for the treatment of hypercholesterolemia.

RESULTS

Nogo-B is involved in cholesterol metabolism

Our previous studies have revealed that Nogo-B is involved in TG metabolism[12,14]; however, few studies have focused on whether Nogo-B is involved in cholesterol metabolism. We identified Nogo-B as a risk factor for high cholesterol levels in 407,746 Europeans by Mendelian randomization analysis in genome-wide association studies (GWASs) data (Integrative Epidemiology Unit Open GWAS Project: ebi-a-GCST90013882; Figure 1B). We further explored the correlation between plasma Nogo-B and lipid levels in 304 Chinese adults (Table S3 presents the basic clinical characteristics). Plasma Nogo-B was positively correlated with total cholesterol (TC) and LDL-C levels, but negatively with high-density lipoprotein-cholesterol (HDL-C) levels (Figures 1C–1E). ApoE is an important component of lipoproteins, especially HDL, and participates in lipid metabolism. We found that plasma Nogo-B levels were negatively correlated with ApoE levels (Figure 1F). However, Nogo-B showed no correlation with TGs, lipoprotein Lp(a), and ApoB levels in human plasma (Figures 1G, S1A, and S1B). Then, we fed wild-type mice normal chow (NC) or an HCD for 3 weeks, and mice serum cholesterol rather than TG levels were elevated under 3 weeks of HCD feeding (Figure 1H). To explore whether Nogo-B responds to cholesterol changes in serum, we collected multiple tissues and found that only liver *Nogo-B* mRNA was elevated (Figure 1I). Liver Nogo-B protein and mRNA levels were both increased

Figure 1. Nogo-B is involved in cholesterol metabolism

(A) Through analysis of 407,746 European in GWAS data, human plasma, and HCD-fed mice, we found that Nogo-B is involved in cholesterol metabolism.

(B) In the GWAS data, we found a causal relationship between Nogo and high cholesterol through Mendelian randomization analysis in a cohort of Europeans (Integrative Epidemiology Unit Open GWAS Project: ebi-a-GCST90013882). *$p < 0.05$ by inverse variance weighted test; $n = 407,746$.

(C–G) Plasma samples were collected from 304 Chinese adults to determine the levels of Nogo-B, TC, LDL-C, HDL-C, ApoE, and TG. Correlation between Nogo-B levels and TC (C), LDL-C (D), HDL-C (E), ApoE (F), and TG (G) was assessed by Pearson's correlation assay. r: correlation coefficient, *p*: *p* value by t test; $n = 304$.

(H–J) C57BL/6J mice were fed with NC and HCD for 3 weeks. (H) Serum TC, LDL-C, and TG levels were determined by enzymatic kits. Data are presented as mean ± SD, ***$p < 0.001$ and ns (not significant) by Student's t test; $n = 7$. (I) Aorta, heart, liver, intestine, kidney, brown adipose tissue (BAT), white adipose tissue (WAT), and muscle tissues were collected, and Nogo-B mRNA levels were determined by qRT-PCR. Data are presented as mean ± SD; ***$p < 0.001$ by Student's t test; ns, not significant; $n = 7$. (J) Protein ($n = 3$) and mRNA ($n = 7$) levels of Nogo-B were determined by western blot and qRT-PCR. Data are presented as mean ± SD; **$p < 0.01$ and ***$p < 0.001$ by Student's t test.

(K–N) NC- or HCD-fed littermate control ($Nogo^{+/+}$) and Nogo-B deficient ($Nogo^{-/-}$) mice serum was determined for TC (K), LDL-C (L), HDL-C (M), and TG (N) levels. Data are presented as mean ± SD; *$p < 0.05$; **$p < 0.01$; ***$p < 0.001$; and ns, not significant by Student's t test; NC group: $n = 6$; HCD group: $n = 7$.

(O and Q) Total RNA prepared from NC- and HCD-fed mice liver were determined for mRNA levels of *HMGCR*, *ABCA1*, *ABCG1*, *ABCG5*, *ABCG8*, *LDLR*, and *ApoE*. Data are presented as mean ± SD; *$p < 0.05$; **$p < 0.01$; ***$p < 0.001$; and ns, not significant by Student's t test; NC group: $n = 5$; HCD group: $n = 6$.

(P) Protein levels of ABCA1, ABCG1, ApoE, LDLR, and SREBP2 (p/m: precursor or mature form of SREBP2) in the NC-fed mice liver were determined by western blot; $n = 4$.

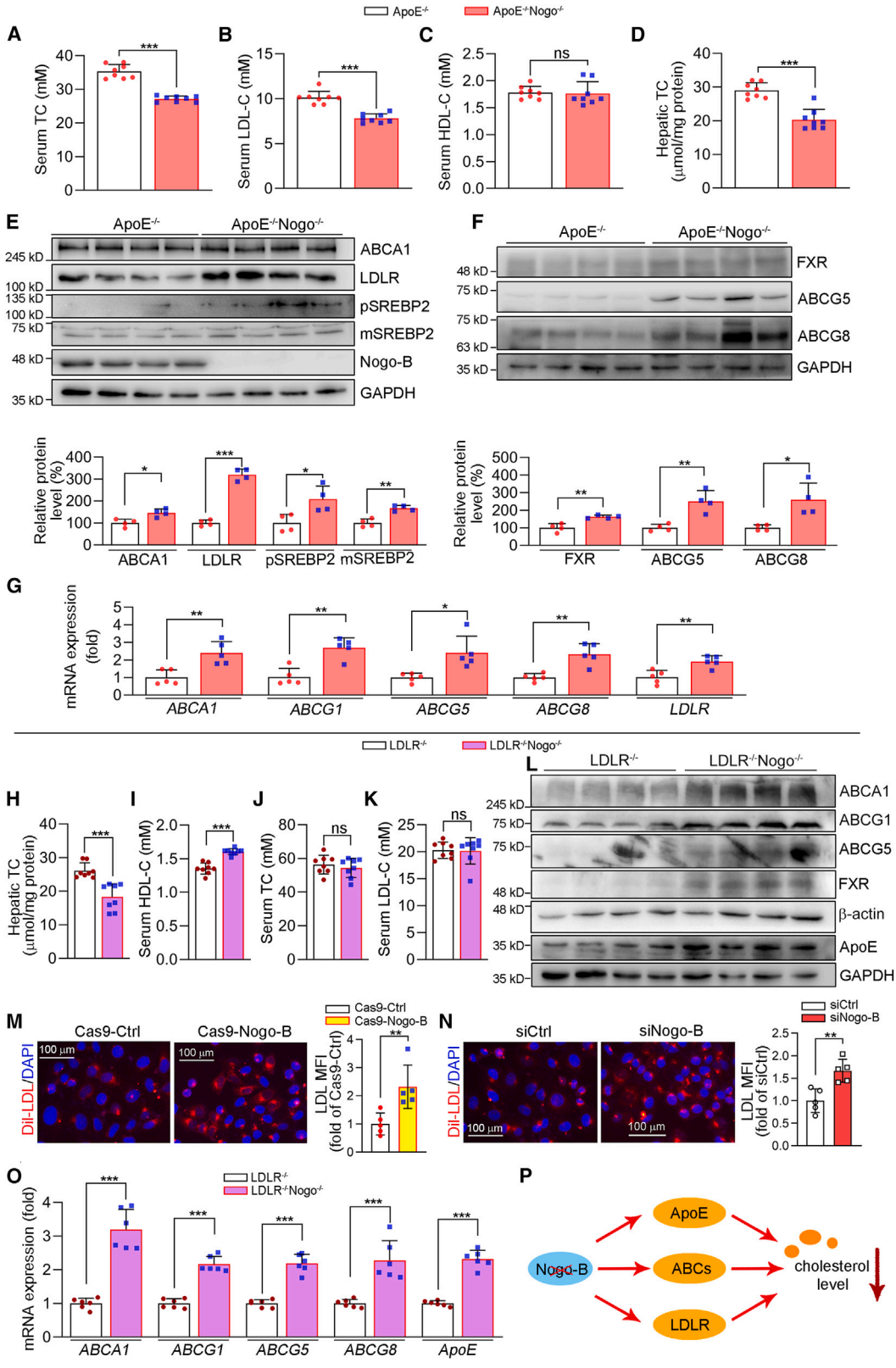

(legend on next page)

under HCD feeding (Figure 1J). These findings suggest that Nogo-B is related to changes in cholesterol levels in humans and mice.

The correlation between Nogo-B and cholesterol levels prompted us to investigate the role of Nogo-B in hypercholesterolemia induced by a HCD. Nogo-B deficiency ($Nogo^{-/-}$) mice and littermate control ($Nogo^{+/+}$) mice were fed with NC or HCD for 3 weeks. To examine the potential role of Nogo-B in cholesterol metabolism, we assessed serum lipid profiles. HCD significantly increased TC levels in serum (Figure 1K). $Nogo^{-/-}$ mice had reduced TC levels only in HCD-fed mice, with no change in NC-fed mice. Interestingly, Nogo-B deficiency decreased levels of LDL-C and increased HDL-C both in NC and HCD-fed mice (Figures 1K–1M). We observed no changes in TG levels in $Nogo^{-/-}$ mice (Figure 1N). Nogo-B deficiency did not induce any obvious liver damage, as evidenced by the unchanged levels of serum aspartate aminotransferase, alanine aminotransferase, and alkaline phosphatase (Table S5). Nogo-B deficiency upregulated mRNA expression of the genes for cholesterol excretion (*ABCA1/G1/G5/G8*), hepatic uptake for cholesterol (*LDLR*), and apolipoprotein (*ApoE*) both in NC and HCD-fed mice (Figures 1O and Q). Protein expression of ABCA1/G1, LDLR, SREBP2, ApoE, and farnesoid X receptor (FXR) was increased in the liver of NC-fed $Nogo^{-/-}$ mice (Figures 1P, S1C, and S1D). However, Nogo-B deficiency has no effect on cholesterol biosynthesis-related gene (HMGCR) expression (Figures 1O, 1Q, S1F, and S1G). It has been reported that FXR activation inhibited cholesterol biosynthesis by inhibiting HMGCR expression,[16] and in turn, Nogo-B deficiency had no effect on HMGCR expression due to the activation of FXR (Figures 1O, 1Q, S1D, S1F, and S1G). Due to the Nogo members sharing the same transcript, we used the term Nogo-B for blood and hepatocytes, and Nogo for animals in this study.[12]

The liver is an important site for cholesterol metabolism. The main process of cholesterol metabolism is (1) transport of cholesterol: endogenous or exogenous cholesterol is loaded on ApoE-containing lipoproteins; (2) liver uptake of cholesterol: LDL, a cholesterol-rich lipoprotein, can be recognized by LDLR and taken up into the liver; and (3) the excretion of cholesterol: liver cholesterol can be metabolized into bile acids or excreted into peripheral tissues through ABCs and eventually excreted into the feces. Through analysis of 407,746 European in GWAS data, human plasma, and HCD-fed mice, we find that Nogo-B is involved in cholesterol metabolism (Figure 1A). Our findings suggest that Nogo-B deficiency lowered cholesterol levels by promoting cholesterol metabolism via enhancing ApoE, LDLR, and ABCs expression.

The benefits of Nogo-B deficiency in improving hyperlipidemia are impaired in $ApoE^{-/-}$ mice

In mice fed a NC diet and HCD, Nogo-B deficiency enhanced ApoE and LDLR protein expression and decreased cholesterol levels. To further investigate the mechanism of metabolic benefits of Nogo-B deficiency, ApoE and Nogo-B double-knockout ($ApoE^{-/-}Nogo^{-/-}$) mice and $ApoE^{-/-}$ mice were fed an HCD for 16 weeks. No differences in food intake or water drinking were observed between the two groups, but the $ApoE^{-/-}Nogo^{-/-}$ mice had a reduced gain in body weight compared with $ApoE^{-/-}$ mice (Table S4).

The serum TC and LDL-C levels were significantly lower in $ApoE^{-/-}Nogo^{-/-}$ mice than those in $ApoE^{-/-}$ mice (Figures 2A and 2B), while HDL-C levels did not differ between the two groups (Figure 2C). Nogo-B deficiency also substantially decreased hepatic cholesterol levels and alleviated HCD-induced liver damage (Figure 2D; Table S5). Moreover, the expression of genes related to cholesterol metabolism, including ABCA1, LDLR, SREBP2, FXR, ABCG5, and ABCG8, was significantly increased in the livers of $ApoE^{-/-}Nogo^{-/-}$ mice (Figures 2E–2G). Figures 1O–1Q show that Nogo-B deficiency activated ApoE expression in $Nogo^{-/-}$ mice liver, and ApoE is an important component of HDL, an atherosclerosis-prevention lipoprotein promoting cholesterol metabolism. The absence of Nogo-B in $ApoE^{-/-}$ mice has no effect on HDL-C (Figure 2C), which might be related to ApoE.

The benefits of Nogo-B deficiency in improving hyperlipidemia are impaired in $LDLR^{-/-}$ mice

To further investigate the role of Nogo-B deficiency in regulating hypercholesterolemia, LDLR and Nogo-B double-knockout ($LDLR^{-/-}Nogo^{-/-}$) mice were generated and fed an HCD for 16 weeks. Unlike $ApoE^{-/-}Nogo^{-/-}$ mice, gains in body weight were similar between $LDLR^{-/-}Nogo^{-/-}$ and $LDLR^{-/-}$ mice (Table S4).

Figure 2. Nogo-B deficiency decreases cholesterol levels related to ApoE, LDLR, and ABCs

(A–G) Blood and liver samples collected from 16-week HCD-fed $ApoE^{-/-}$ and $ApoE^{-/-}Nogo^{-/-}$ male mice were used for the following assays: (A–C) Serum TC (A), LDL-C (B), and HDL-C (C) levels were determined by enzymatic kits. Data are presented as mean ± SD; ***$p < 0.001$; ns, not significant by Student's t test; $n = 8$. (D) Liver TC content was determined by an assay kit. Data are presented as mean ± SD; ***$p < 0.001$ by Student's t test; $n = 8$. (E and F) Protein expression of ABCA1, LDLR, (p/m) SREBP2 and Nogo-B (E), and FXR, ABCG5, and ABCG8 (F) with quantitation of band density correspondingly. Data are presented as mean ± SD; *$p < 0.05$; **$p < 0.01$; ***$p < 0.001$ by Student's t test; $n = 4$. (G) mRNA expression of *ABCA1*, *ABCG1*, *ABCG5*, *ABCG8*, and *LDLR* in the liver was determined by qRT-PCR. Data are presented as mean ± SD; *$p < 0.05$ and **$p < 0.01$ by Student's t test; $n = 5$.

(H–O) $LDLR^{-/-}$ and $LDLR^{-/-}Nogo^{-/-}$ male mice fed with HCD for 16 weeks, and serum and liver samples were used for the following assays: (H) Hepatic TC levels were determined by an assay kit. Data are presented as mean ± SD; ***$p < 0.001$ by Student's t test; $n = 8$. (I–K) Serum HDL-C (I), TC (J), and LDL-C (K) were determined by enzymatic kits. Data are presented as mean ± SD; ***$p < 0.001$; and ns, not significant by Student's t test; $n = 8$. (L) Liver protein expression of ABCA1, ABCG1/5, FXR, and ApoE was determined by western blot. $n = 4$. (M and N) HepG2 cells were transfected with si-Ctrl or si-Nogo-B as indicated for 24 h, followed by culture in complete medium for another 24 h. Cas9-Ctrl, Cas9-Nogo-B cells, or siRNA-transfected HepG2 cells were incubated with 3,3′-dioctadecylindocarbocyanine (DiI)-LDL (20 μg/mL) for 4 h. After staining with DAPI for nucleus, the binding/internalized DiI-LDL was observed and captured with a Leica microscope (M and N). Scale bar, 100 μm. Data are presented as mean ± SD; **$p < 0.01$ by Student's t test; $n = 5$. (O) Liver mRNA levels of *ABCA1*, *ABCG1/5/8*, and *ApoE* were determined by qRT-PCR. Data are presented as mean ± SD; ***$p < 0.001$ by Student's t test; $n = 6$.

(P) Nogo-B deficiency decreased the cholesterol level by activating ApoE, LDLR, and ABCs expression.

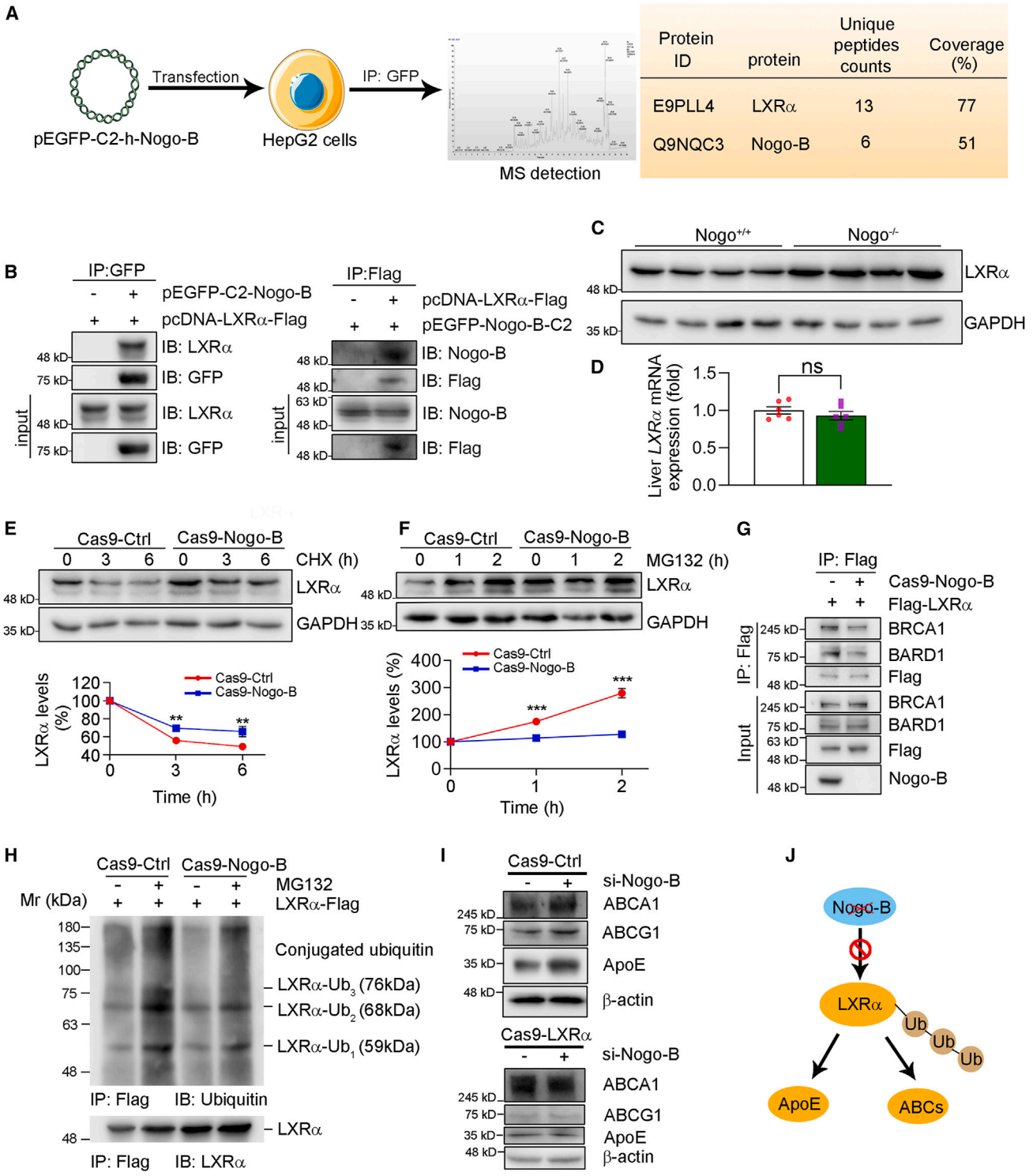

Figure 3. Nogo-B deficiency activates LXRα by enhancing LXRα protein stability

(A) Cellular proteins of HepG2 cells transfected with pEGFP-C2-h-Nogo-B were purified by IP with anti-GFP antibody and subjected to mass spectrometry assay. Total ion chromatograph is shown. LXRα was identified for candidate proteins interacting with Nogo-B.

(B) We transfected 293T cells with pEGFP-C2-Nogo-B plus pcDNA3-LXRα-FLAG expression vectors, followed by IP using anti-GFP or anti-FLAG antibody, SDS-PAGE, and immunoblotting using anti-GFP and LXRα or anti-Nogo-B and FLAG antibodies.

(legend continued on next page)

Hepatic TC levels were decreased in LDLR$^{-/-}$Nogo$^{-/-}$ mice (Figure 2H), and liver cholesterol metabolism-related genes, including ABCA1/G1/G5/G8, ApoE, and FXR, were activated by Nogo-B deficiency (Figures 2L, 2O, and S2). Interestingly, Nogo-B deficiency increased HDL-C levels (Figure 2I). However, Nogo-B deficiency had no effect on TC and LDL-C levels (Figures 2J and 2K). LDL-C clearance mediated by LDLR in the liver is an essential process to improve cholesterol profiles.[17] Uptake of LDL-C by Nogo-B knockout- or Nogo-B siRNA (si-Nogo-B)-transfected HepG2 cells was enhanced by activating LDLR expression (Figures 1P, 2E, 2M, 2N, and 2P). The absence of Nogo-B in LDLR$^{-/-}$ mice has no effect on TC and LDL-C (Figures 2J and 2K), which might be related to LDLR.

Combining the above results, the improved cholesterol metabolism by Nogo-B deficiency might require ApoE and LDLR presence, accompanied by the increased expression of ABCA1/G1/G5/G8 in ApoE$^{-/-}$ and LDLR$^{-/-}$ mice simultaneously (Figure 2P).

Interactions between Nogo-B and LXRα facilitate LXRα degradation

To investigate the mechanism underlying the regulation of ABCA1/G1/G5/G8, ApoE, and LDLR expression by Nogo-B deficiency, we screened for candidate proteins that can bind with Nogo-B in HepG2 cells using mass spectrometry (Figure 3A). We identified LXRα, the master transcription factors of ABCA1/G1/G5/G8 and ApoE and the main subtype of LXRs present in the liver (Figure 3A). The interaction between Nogo-B and LXRα was further confirmed by co-immunoprecipitation (coIP) assay (Figures 3B and S3A), and significant cellular colocalization was observed between Nogo-B and LXRα in HepG2 cells (Figure S3B). Interestingly, Nogo-B deficiency did not affect *LXRα* mRNA expression, but it did increase LXRα protein levels in the liver of mice fed a 3-week HCD (Figures 3C and 3D). This suggests that Nogo-B is involved in the post-transcriptional regulation of LXRα rather than transcriptional regulation. Correspondingly, protein levels of LXRα were increased in ApoE$^{-/-}$Nogo$^{-/-}$ mice (Figure S3C).

Hsieh et al. have identified LXRα as subject to ubiquitin-mediated protein degradation.[18] To determine whether Nogo-B is required for maintaining LXRα protein stability, HepG2 cells were treated with cycloheximide (CHX), an inhibitor of protein synthesis. Figure 3E shows that Nogo-B$^{-/-}$ in cells (Cas9-Nogo-B) appropriately maintained LXRα protein stability. Protein degradation is mainly mediated by the autophagy or ubiquitination pathway.[19] MG132 (a proteasome inhibitor), but not 3-methyladenine (an autophagy inhibitor), abolished the elevation of LXRα protein by Nogo-B deficiency (Figures 3F and S3D), suggesting that proteasome-mediated degradation but not the autophagy pathway is involved in LXRα protein stability. Proteasome-mediated protein degradation depends on the ubiquitination pathway.[20] Indeed, Nogo-B deficiency clearly lowered polyubiquitinated LXRα in HepG2 cells (Figure 3H). The ubiquitination degradation of LXRα was mediated by E3 ubiquitin ligase breast cancer-associated protein 1 (BRCA1) and BRCA1-associated RING domain protein 1 (BARD1).[21] Interestingly, the combination of LXRα and BRCA1 and BARD1 was decreased in Nogo-B deficient HepG2 cells (Figure 3G). In addition, we found that inhibiting Nogo-B expression did not increase ABCA1, ABCG1, and ApoE expression in LXRα knockout HepG2 cells (Figure 3I), implying that Nogo-B regulates ABCs and ApoE expression requiring LXRα. These findings suggest that Nogo-B deficiency inhibits the ubiquitin-mediated LXRα degradation (Figure 3J).

Nogo-B deficiency decreases cholesterol levels but does not affect TG levels involving FXR activation

As shown by the above results, Nogo-B deficiency promotes the expression of the cholesterol excretion-related genes, ABCs, by elevating LXRα protein levels (Figures 1P, 4A, and S4A). Correspondingly, Nogo-B deficiency reduced serum and liver cholesterol levels but increased fecal cholesterol levels in 3-week HCD-fed mice (Figures 1K, 4B, and 4C). It has been reported that the activation of LXRα enhances hepatic lipogenesis by upregulating SREBP1 and its targeted genes, such as acyl-coenzyme A (CoA) carboxylase 1 (ACC1), fatty acid synthase (FASN), and stearoyl-CoA desaturase-1 (SCD1).[22] However, despite the significant activation of LXRα by Nogo-B deficiency, liver and serum TG levels were not affected in Nogo$^{-/-}$ mice fed a 3-week HCD (Figures 1N, 4D, and 4E). These results prompted us to explore the mechanism by which Nogo-B deficiency did not increase TG levels despite the activation of LXRα.

Previous studies have shown that activation of FXR represses the activation of SREBP1 and its target genes by LXRα, while having no effect on genes involved in cholesterol metabolism, including ABCA1, ABCG5, and ABCG8.[23] It has been reported that Nogo-B deficiency activated FXR expression,[24] and we found that Nogo-B deficiency in 3-week HCD-fed mice induced liver FXR expression (Figure 4G). Consequently, Nogo-B deficiency had no effect on SREBP1, ACC1, FASN, and SCD1 expression, but it still activated ABCA1/G1/5/8 and ApoE expression in the liver of 3-week HCD-fed mice (Figures 1Q, 4F, and 4G). These results suggest that the deletion of Nogo-B

(C and D) Liver samples collected from 3-week HCD-fed mice were determined for the expression of LXRα protein (C, $n = 4$) and mRNA (D, $n = 6$). Data are presented as mean ± SD; ns, not significant by Student's t test.

(E and F) Cas9-Ctrl and Cas9-Nogo-B HepG2 cells were treated with CHX (100 μg/mL, E) or MG132 (10 μM, F) for the indicated times, followed by determination of LXRα protein expression. Comparison between Cas9-Nogo-B and the corresponding Cas9-Ctrl. Data are presented as mean ± SD; $^{**}p < 0.01$ and $^{***}p < 0.001$ by Student's t test; $n = 3$.

(G) Cas9-Ctrl and Cas9-Nogo-B HepG2 cells were transfected with FLAG-LXRα plasmid, followed by IP with FLAG antibody and immunoblotted with BRCA1, BARD1, FLAG, and Nogo-B antibodies.

(H) LXRα-transfected Cas9-Ctrl and Cas9-Nogo-B HepG2 cells were treated with MG132 (10 μM) for 2 h, followed by IP using anti-FLAG antibody and immunoblotting using anti-ubiquitin and anti-LXRα antibodies.

(I) LXRα-deficient HepG2 cells (Cas9-LXRα) and corresponding control cells (Cas9-Ctrl) were transfected with Nogo-B or control siRNA for 24 h as indicated, and then the protein was extracted and detected for ABCA1, ABCG1, and ApoE expression.

(J) Nogo-B deficiency inhibited the ubiquitination of LXRα, thereby increasing LXRα protein levels.

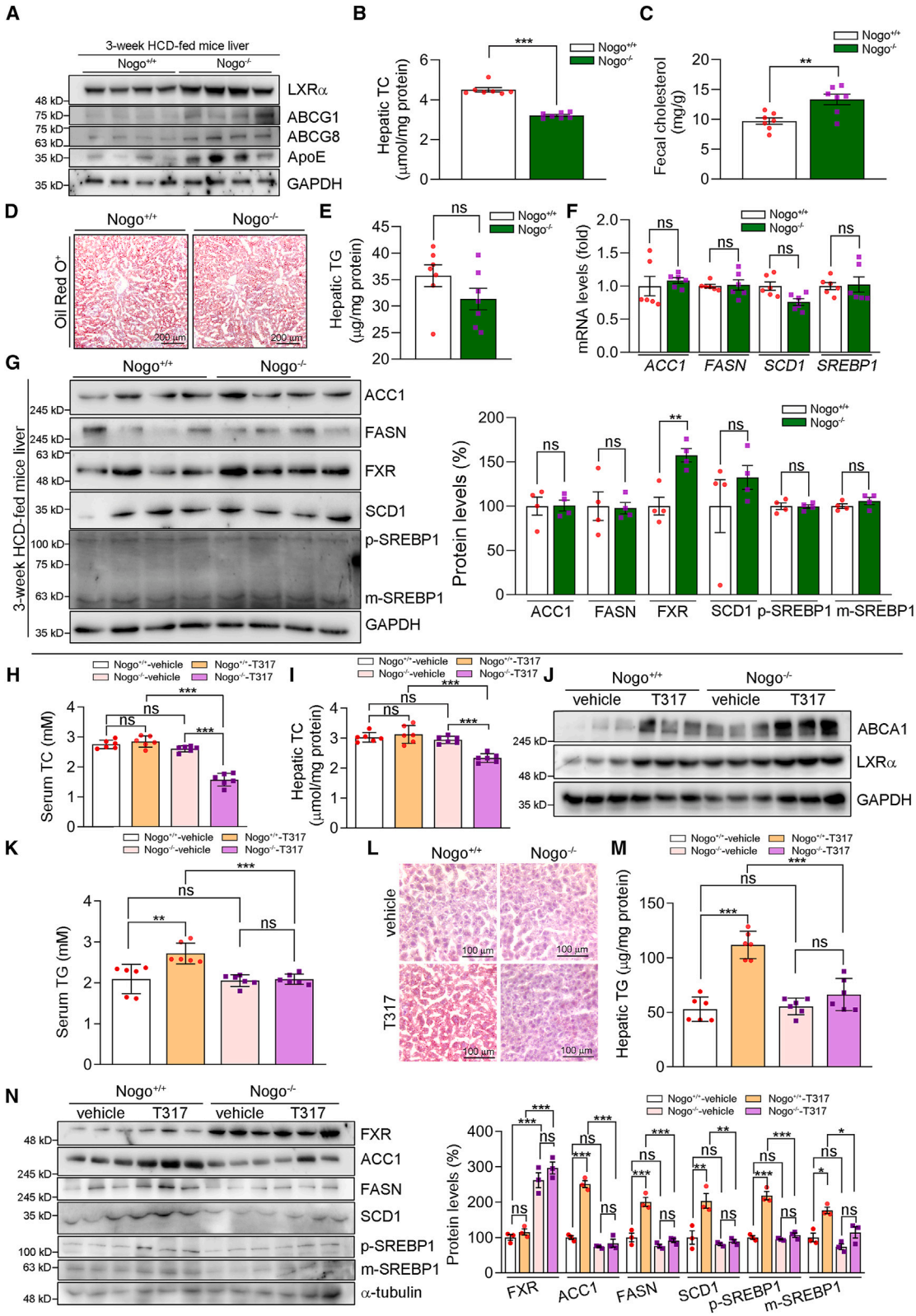

Figure 4. Nogo-B deficiency decreases cholesterol levels without increasing TG levels involving activating FXR expression

(A–G) The liver samples of 3-week HCD-fed male mice were conducted with the following assays: (A and G) liver protein levels of LXRα, ABCG1, ABCG8, and ApoE (A), and ACC1, FASN, FXR, SCD1, and (p/m) SREBP1 (G) were determined by western blot. Data are presented as mean ± SD; $^{**}p < 0.01$; and ns, not

(legend continued on next page)

does not result in lipogenesis, which involves the activation of FXR.

Nogo-B deficiency reduces cholesterol levels without increasing TG levels under LXRα ligand treatment

To further explore whether Nogo-B deficiency can antagonize lipogenesis caused by LXRα activation, we used T0901317 (T317), a synthetic ligand for activating LXRα to treat NC-fed Nogo$^{+/+}$ and Nogo$^{-/-}$ mice. Interestingly, we found that T317 did not affect serum and liver cholesterol levels in Nogo$^{+/+}$ mice under LXRα activation, but T317 did reduce cholesterol levels in Nogo-B-deficient mice (Figures 4H–4J, S4B,and S4C). In addition, we found that T317 increased serum TG levels by approximately 30% in Nogo$^{+/+}$ mice, but this effect was completely blocked in Nogo$^{-/-}$ mice (Figure 4K). T317 also substantially increased neutral lipid and TG content in the liver of Nogo$^{+/+}$ mice, but this was remarkably blocked by Nogo$^{-/-}$ (Figures 4L and 4M). At the molecular level, T317 activated the expression of lipogenic genes (ACC1, FASN, SCD1, and SREBP1) in Nogo$^{+/+}$ mice livers, but it had little effect on them in Nogo$^{-/-}$ mice livers with the activation of FXR expression (Figures 4N and S4C). Interestingly, Nogo$^{-/-}$ increased FXR expression, which was not impacted by T317 treatment (Figure 4N). These results suggest that Nogo-B deficiency further reduces cholesterol levels but does not increase TG levels under LXRα ligand treatment.

To investigate whether the inhibition of LXRα-SREBP1 by Nogo-B deficiency depends on FXR activation, we treated HepG2 cells with T317. T317 increased intracellular lipid content in Cas9-Ctrl (control) cells, which was totally abolished in Cas9-Nogo-B cells (Figures S4D and S4E). Furthermore, the anti-lipogenic effects of Nogo-B deficiency were reversed by FXR siRNA, resulting in higher lipid levels compared to T317-treated Cas9-Ctrl cells (Figures S4D and S4E). Meanwhile, mRNA levels of *SREBP1*, *ACC1*, *FASN*, and *SCD1* were significantly activated by FXR siRNA in Cas9-Nogo-B cells, suggesting that Nogo-B deficiency inhibits the LXRα-SREBP1 pathway requiring FXR (Figure S4F). These findings suggest that Nogo-B deficiency inhibits the LXRα-SREBP1 pathway requiring the activation of FXR (Figure S4G).

Nogo-B inhibition reduces established plaques in ApoE$^{+/-}$LDLR$^{+/-}$ mice

Hypercholesterolemia is a major risk factor for atherosclerosis. To investigate whether Nogo-B regulates the progression of the formation of plaques, we isolated aortas from the ApoE$^{-/-}$ and ApoE$^{-/-}$Nogo$^{-/-}$ or LDLR$^{-/-}$ and LDLR$^{-/-}$Nogo$^{-/-}$ mice shown in Figure 2. As shown in Figure 2, Nogo-B deficiency only decreased TC and LDL-C levels in ApoE$^{-/-}$ mice and only increased HDL-C levels in LDLR$^{-/-}$ mice. Consistent with the incomplete anti-hypercholesterolemia ability of ApoE$^{-/-}$Nogo$^{-/-}$ and LDLR$^{-/-}$Nogo$^{-/-}$ mice, Nogo-B deficiency only suppressed plaques areas in the abdominal aorta without affecting the aortic arch and thoracic aorta (Figures 5A, 5B, S5A, and S5B). These findings suggest that Nogo-B deficiency is required for the presence of ApoE and LDLR to exert its anti-hypercholesterolemia and anti-atherogenic plaques properties. Based on this finding, ApoE and LDLR dual heterozygote (ApoE$^{+/-}$LDLR$^{+/-}$) mice were constructed.

ApoE$^{+/-}$LDLR$^{+/-}$ mice were fed an HCD for 20 weeks and then intravenously injected with control siRNA (si-Ctrl) or Nogo-B siRNA (si-Nogo-B) for 6 weeks (Figure 5C). Surprisingly, the inhibition of Nogo-B expression by Nogo-B siRNA not only reduced abdominal aortic plaques but also reduced total aortic plaques (Figure 5D). Nogo-B inhibition also decreased aortic sinus lesions and oil red O^{+} areas in ApoE$^{+/-}$LDLR$^{+/-}$ mice with established lesions (Figures 5E and S5E). si-Nogo-B also increased fibrotic caps in the aortic sinus (Figures 5F and S5F). These findings suggest that inhibiting Nogo-B expression exerts a better anti-atherosclerotic plaques effect in the presence of ApoE and LDLR.

Nogo-B inhibition decreases cholesterol levels in ApoE$^{+/-}$LDLR$^{+/-}$ mice

The anti-atherosclerotic plaques properties of Nogo-B inhibition in ApoE$^{+/-}$LDLR$^{+/-}$ mice prompted us to investigate changes in cholesterol levels. Nogo-B inhibition substantially reduced serum TC and LDL-C, but increased HDL-C levels in ApoE$^{+/-}$LDLR$^{+/-}$ mice (Figure 5H). Additionally, hepatic cholesterol content was decreased by Nogo-B inhibition (Figure 5I), and fecal cholesterol levels were increased (Figure 5J). The decreased cholesterol levels in liver should be attributed to the activated expression of LXRα, ApoE, ABCA1/G1/G5/G8, LDLR, and FXR by si-Nogo-B (Figures 5K and 5L). Overall, the benefits of Nogo-B inhibition on lowering cholesterol levels and reducing atherosclerotic plaques should be attributed to the activation of ABCs, ApoE, and LDLR.

We found that Nogo-B siRNA mainly inhibited the expression of Nogo-B in the liver and had little effect on other tissues (Figures 5G, S5C, and S5D), implying that liver Nogo-B played an important role in cholesterol metabolism.

Liver Nogo-B inhibition decreases cholesterol levels

To further confirm the role of Nogo-B in regulating cholesterol metabolism in the liver, we used adeno-associated virus

significant by Student's t test; $n = 4$. (B and C) Hepatic (B) and fecal (C) cholesterol levels were determined by assay kits. Data are presented as mean ± SD; $^{**}p < 0.01$ and $^{***}p < 0.001$ by Student's t test; $n = 7$. (D) Oil red O staining of liver frozen sections. Scale bar, 200 μm. (E) Hepatic TG levels were determined by an assay kit. Data are presented as mean ± SD; ns, not significant by Student's t test; $n = 7$. (F) Liver mRNA expression of *ACC1*, *FASN*, *SCD1*, and *SREBP1* were determined by qRT-PCR. Data are presented as mean ± SD; ns, not significant by Student's t test; $n = 6$.

(H–N) NC-fed Nogo$^{+/+}$ and Nogo$^{-/-}$ male mice received oral administration of T0901317 at 1 mg/kg body weight/day for 9 days. After treatment, mouse blood and liver samples were collected for the following assays: (H and K) serum TC (H) and TG (K) levels were determined by assay kits. Data are presented as mean ± SD; $^{**}p < 0.01$; $^{***}p < 0.001$; and ns, not significant by two-way ANOVA; $n = 6$. (I and M) Hepatic cholesterol (I) and TG (M) levels were determined by assay kits. Data are presented as mean ± SD; $^{***}p < 0.001$; and ns, not significant by two-way ANOVA; $n = 6$. (L) Hepatic lipid content was determined by oil red O staining of liver frozen sections. Scale bar, 100 μm. (J and N) Protein expression of ABCA1 and LXRα (J), and FXR, ACC1, FASN, SCD1, and (p/m) SREBP1 in mouse liver (N) was determined by western blot. Data are presented as mean ± SD; $^{*}p < 0.05$; $^{**}p < 0.01$; $^{***}p < 0.001$; and ns, not significant by two-way ANOVA; $n = 3$.

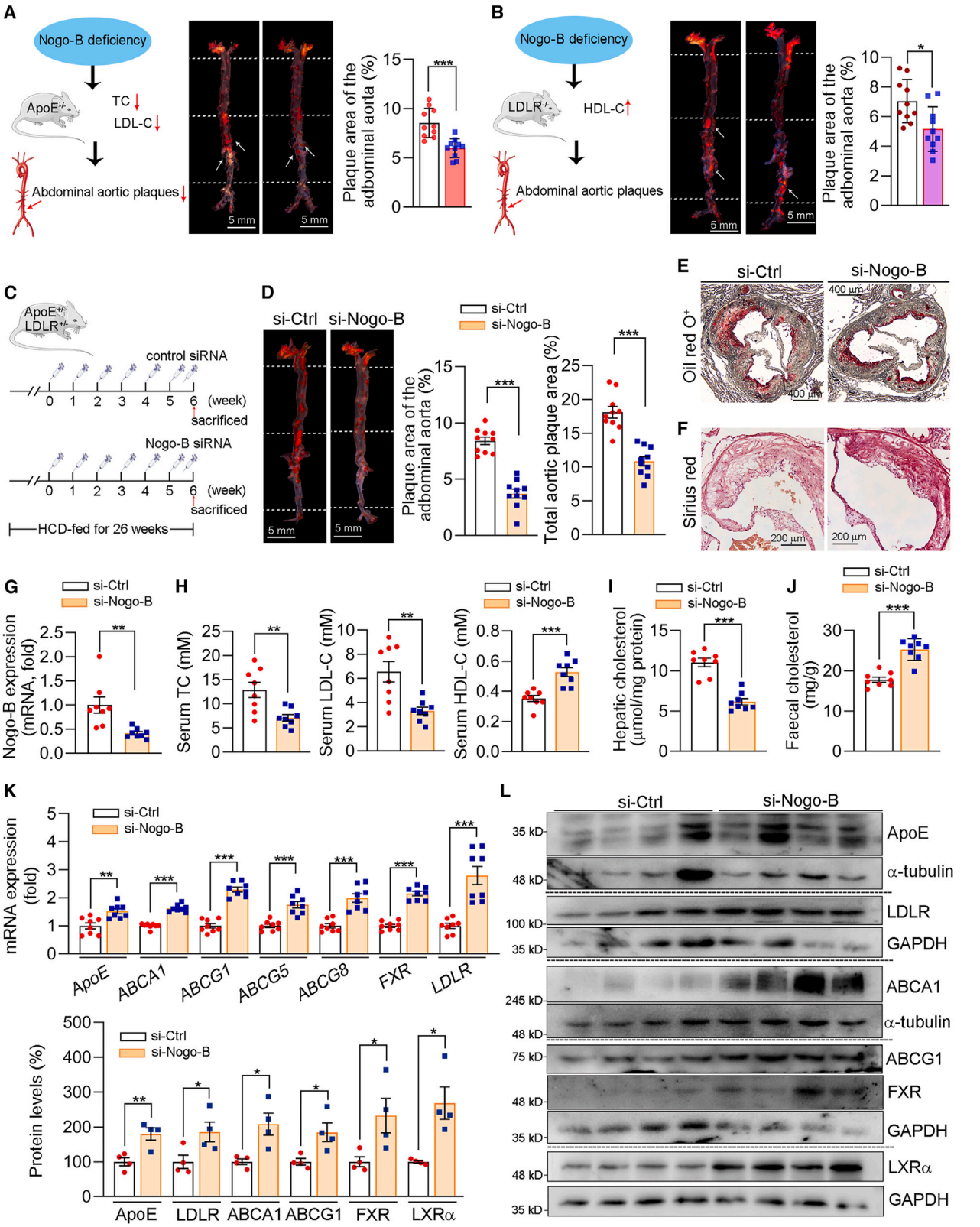

(legend on next page)

8/thyroxin binding globulin-small hairpin RNA (AAV8-TBG-shRNA) to inhibit Nogo-B expression in mice liver. Mice intravenously injected with AAV8-TBG-shNogo-B exhibited decreased liver Nogo-B expression, with no changes in other tissues (Figures 6A, S6A, and S6B). Hepatic Nogo-B inhibition exhibited decreased serum TC, LDL-C, and increased HDL-C levels (Figure 6B). In line with serum lipid levels, hepatic cholesterol levels were decreased by hepatic Nogo-B inhibition accompanied by the activation of LXRα, FXR, ApoE, ABCs, SREBP2, and LDLR expression (Figures 6C, 6E–6G, S6C). Inhibiting Nogo-B expression has no effect on the TC levels in bile, but it does increase bile acid levels (Figures S6D and S6E). Ultimately, due to the activation of cholesterol excretion, the cholesterol level in feces was increased in Nogo-B-inhibited mice (Figure 6D). Inhibition of Nogo-B expression had no effect on liver lipogenesis genes expression by the activation of FXR (Figures 6E–6G and S6C). These findings suggest that liver Nogo-B plays a vital role in lowering cholesterol levels.

Nogo-B is associated with cholesterol abnormality and atherosclerosis in humans

Abnormal cholesterol metabolism is one of the major risk factors for atherosclerotic cardiovascular disease (ASCVD) in humans.[25] We collected blood samples from 65 normal volunteers (defined as individuals with no atherosclerotic plaques in the coronary artery) and 239 patients with atherosclerosis (Table S3 presents the basic clinical characteristics). Compared with normal volunteers, we found that atherosclerotic patients exhibit higher cholesterol levels (Figure 6H), suggesting the existence of abnormalities in cholesterol metabolism in these patients with atherosclerosis. We found that plasma Nogo-B levels were approximately 1.7-fold higher in atherosclerotic patients compared to normal volunteers (Figure 6I). Correspondingly, in patients with atherosclerosis accompanied by abnormal cholesterol metabolism, we also found that Nogo-B levels were positively correlated with TC and LDL-C levels, and negatively correlated with HDL-C levels (Figures 6J–6L). Additionally, we observed that plasma ApoE levels were negatively correlated with Nogo-B levels in atherosclerotic patients (Figure 6M). Combined with Figures 1C–1F, these results indicate that Nogo-B is tightly associated with cholesterol levels in human plasma and associated with abnormal cholesterol metabolism and ASCVD in humans.

DISCUSSION

Our previous study had shown that Nogo-B receptor (NgBR) promoted LXRα nuclear translocation and hepatic lipid accumulation.[26] However, our subsequent studies found that Nogo-B exerted its functions without affecting the expression of its receptor NgBR.[12,14] In this study, we found that Nogo-B directly interacted with LXRα and participated in its ubiquitination degradation, which suggested that Nogo-B regulated LXRα protein levels independently of NgBR. It has been reported that AMP-activated protein kinase (AMPK) regulates the ubiquitin-mediated degradation of LXR through BRCA1.[21] Nogo-B deficiency promoted lipid oxidation through AMPK,[14] suggesting that Nogo-B might regulate the ubiquitination process of LXRα via AMPK.

In hepatocytes, Nogo-B deficiency activates cholesterol transport and reduces liver/cellular cholesterol levels. This activation, in turn, activates SREBP2 expression, resulting in increased LDLR expression and enhanced LDL uptake. It is well established that SREBP2 is able to strongly activate the expression of HMGCR, the rate-limiting enzyme for cholesterol synthesis. High expression of FXR inhibited cholesterol synthesis by decreasing HMGCR expression.[16] Other studies indicated that FXR may repress the expression of HMGCR through the disruption of the functional CREB/CRT2 complex,[27,28] which may have resulted in no change in HMGCR expression by Nogo-B deficiency. Phosphorylation abolishes HMGCR activity.[29] It has been reported that HMGCR is primarily phosphorylated by AMPK.[30] Interestingly, our previous study showed that Nogo-B deficiency activated AMPK expression.[14] This suggests that Nogo-B may inhibit HMGCR activity by activating AMPK. In mice fed an NC diet, Nogo-B deficiency did not affect serum TC levels, which may be due to the reduction in LDL-C levels and the increase in HDL-C levels caused by Nogo-B deficiency, with the values of LDL-C and HDL-C being relatively close. However, HCD significantly induces an increase in LDL-C levels, and Nogo-B deficiency has been shown to reduce total serum cholesterol levels.

It has been reported that hepatic ABCA1 activation leads to an increase in HDL-C levels.[31,32] However, in our study, Nogo-B deficiency did not increase HDL-C levels in ApoE$^{-/-}$ mice

Figure 5. Nogo-B inhibition decreases established lesions and cholesterol levels in ApoE$^{+/-}$LDLR$^{+/-}$ mice

(A and B) 16-week HCD-fed mice in Figure 2 aortas were collected and stained with oil red O (A and B, center). Quantitative statistics of abdominal aorta plaques areas (A and B, right; arrows: atherosclerotic plaques). Scale bar, 5 mm. Data are presented as mean ± SD; *$p < 0.05$ and ***$p < 0.001$ by Student's t test; $n = 10$.

(C) ApoE$^{+/-}$LDLR$^{+/-}$ dual heterozygote male mice were fed HCD for 20 weeks, then divided into two groups randomly and intravenously injected control (si-Ctrl) and Nogo-B siRNA (si-Nogo-B), respectively, for 6 weeks (once per week for the first 5 weeks and twice for the last week). After treatment, aortas, serum, and liver samples were conducted the following assays (D–L).

(D) *En face* aortic lesions were stained by oil red O. The proportions of plaques in the total aorta and abdominal aorta were quantitatively analyzed separately. Scale bar, 5 mm. Data are presented as mean ± SD; ***$p < 0.001$ by Student's t test; $n = 10$.

(E) Aortic root sinus lesions were stained by oil red O. Scale bar, 400 μm.

(F) Arterial collagen was stained by Sirius red staining. Scale bar, 200 μm.

(G and K) Liver mRNA levels of *Nogo-B* (G) and *ApoE*, *ABCA1*, *ABCG1*, *ABCG5*, *ABCG8*, *FXR*, and *LDLR* (K) were determined by qRT-PCR. Data are presented as mean ± SD; **$p < 0.01$ and ***$p < 0.001$ by Student's t test; $n = 8$.

(H) Serum TC, LDL-C, and HDL-C levels were determined by assay kits. Data are presented as mean ± SD; **$p < 0.01$ and ***$p < 0.001$ by Student's t test; $n = 8$.

(I and J) Liver (I) and fecal (J) TC contents were determined by assay kits. Data are presented as mean ± SD; ***$p < 0.001$ by Student's t test; $n = 8$.

(L) Liver protein levels of ApoE, LDLR, ABCA1, ABCG1, FXR, and LXRα were determined by western blot with quantitative statistics. Data are presented as mean ± SD; *$p < 0.05$ and **$p < 0.01$ by Student's t test; $n = 4$.

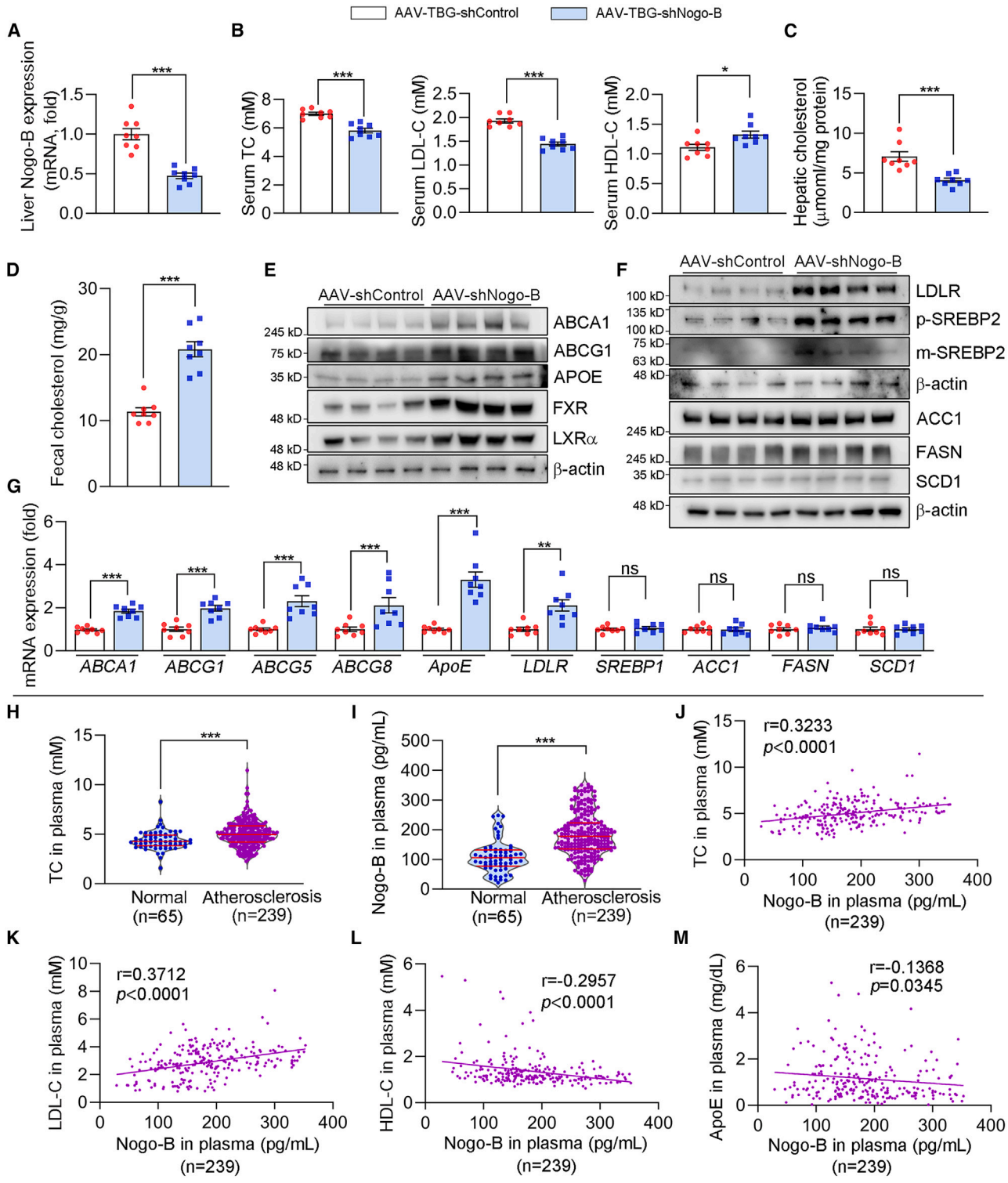

Figure 6. Liver Nogo-B inhibition decreases cholesterol levels

(A–G) To further confirm the role of Nogo-B in regulating cholesterol metabolism in the liver, we used AAV8-TBG-shRNA to inhibit *Nogo-B* expression in mice liver. (A and G) Liver mRNA levels of *Nogo-B* (A) and *ABCA1*, *ABCG1/G5/G8*, *ApoE*, *LDLR*, *SREBP1*, *ACC1*, *FASN*, and *SCD1* (G) were determined by qRT-PCR. Data are presented as mean ± SD; $^{**}p < 0.01$; $^{***}p < 0.001$; and ns, not significant by Student's t test; $n = 8$. (B) Serum TC, LDL-C, and HDL-C levels were determined by assay kits. Data are presented as mean ± SD; $^{*}p < 0.05$ and $^{***}p < 0.001$ by Student's t test; $n = 8$. (C and D) Hepatic (C) and fecal (D) cholesterol levels were

(legend continued on next page)

despite the activation of ABCA1/ABCG1. Since ApoE also plays a crucial role in HDL assembly, this suggests that the effect of Nogo-B on increasing HDL-C levels might be related to ApoE. Therefore, the mechanism by which Nogo-B regulates HDL-C levels requires further investigation. Similarly, the mechanism by which Nogo-B regulates LDL-C levels also needs more work to be elucidated.

In mice injected with AAV-TBG-shRNA, inhibiting hepatic Nogo-B expression was able to decrease liver cholesterol levels and increase fecal cholesterol levels. However, Nogo-B inhibition had no effect on the TC levels in bile. Additionally, our study found that Nogo-B deficiency increased bile acid levels in bile, which is consistent with our previous research.[24] Bile acid acts as a receptor for cholesterol, forming micelles that increase cholesterol saturation in bile and promote its transport to the intestine.[33] Additionally, bile acid facilitates the re-absorption of cholesterol by intestinal NPC1L1. Therefore, bile acids are crucial in facilitating the enterohepatic circulation of bile cholesterol. We speculate that Nogo-B inhibition may promote the circulation of bile cholesterol by increasing bile acid levels. Consequently, Nogo-B inhibition did not raise bile cholesterol levels or cause cholesterol accumulation in bile. However, the specific mechanisms still need further validation.

Several clinical trials indicate that the use of obeticholic acid, an FXR agonist, increases serum TC levels.[34,35] Interestingly, in our study, Nogo-B deficiency decreased serum cholesterol levels while simultaneously activating FXR. It is generally believed that FXR activation inhibits the expression of CYP7A1, a key enzyme in cholesterol catabolism to bile acids, thus leading to cholesterol accumulation and elevating serum cholesterol levels.[36] Our previous study found that Nogo-B deficiency can activate CYP7A1 expression while activating FXR expression.[24] Increasing studies indicate that the intestinal FXR/fibroblast growth factor 15/19 axis is the main suppressor of hepatic CYP7A1 expression, whereas the hepatic FXR/small heterodimer partner pathway shows only minor inhibitory effects.[37] Our study found that Nogo-B does not affect FXR expression in the small intestine. These factors may explain why Nogo-B, despite activating FXR, does not induce an increase in cholesterol levels. However, the specific mechanisms still need to be explored further.

Different from traditional drugs targeting HMGCR and LDLR for ASCVD treatment, such as statins and PCSK9 inhibitors, Nogo-B inhibition can increase not only the LDLR protein level but also ApoE and ABCs expression, exerting a strategy on hypercholesterolemia and atherosclerosis treatment.

The role of LXR in cholesterol metabolism has been increasingly demonstrated. Promoting LXR protein stability and inhibiting the role of LXRα in lipid synthesis have been found to be crucial in enhancing cholesterol metabolism and lowering cholesterol levels. For example, inhibiting ASGR1 expression can suppress LXRα ubiquitination degradation and inhibit LXRα-induced lipid synthesis by activating AMPK, thereby promoting cholesterol excretion.[21] TTC39B deficiency can alleviate steatohepatitis and atherosclerosis by suppressing LXRα ubiquitination degradation and increasing the content of unsaturated fatty acid-containing phospholipids to inhibit LXRα-induced lipid synthesis.[18] Synthetic LXR ligands may have been found to significantly reduce atherosclerosis but they do induce severe lipogenesis and fatty liver, limiting their clinical application.[38] Our study suggests that combining Nogo-B inhibition with LXR ligands may enhance the effects of LXR ligands on cholesterol metabolism while counteracting LXR ligand-induced lipogenesis.

Limitations of the study

One limitation of our study is that we did not identify the specific ubiquitination sites of LXRα. Clarifying these specific ubiquitination sites would provide a better understanding of the regulatory mechanisms of the ubiquitination and degradation of LXRα. Studies have shown that activation of ABCA1 can increase serum HDL-C levels in mice. However, we found that while Nogo-B deficiency in ApoE$^{-/-}$ mice activated ABCA1 expression, it did not increase serum HDL-C levels. This finding differs from other studies and still requires sufficient evidence for validation. In addition, we found that Nogo-B inhibition reduced liver cholesterol levels and increased fecal cholesterol levels, but it had no effect on bile cholesterol levels. We hypothesized that this may be related to the increase in bile acid levels due to Nogo-B inhibition. However, further work is needed to validate this hypothesis. Although we used AAV8-TBG-shRNA to inhibit hepatic Nogo-B expression, we did not use hepatocyte-specific Nogo-B knockout mice, which is also a limitation of our study.

RESOURCE AVAILABILITY

Lead contact

Further information and requests for resources and reagents should be directed to and will be fulfilled by the lead contact, Yajun Duan (yajunduan@ustc.edu.cn).

Materials availability

Nogo$^{-/-}$ mice in C57BL/6JGpt background are available from the lead contact upon request.

Data and code availability

- All data reported in the paper are available from the lead contact upon request.
- This paper does not report original code.
- Any additional information required to reanalyze the data reported in this paper is available from the lead contact upon request.

ACKNOWLEDGMENTS

This work was supported by the National Natural Science Foundation of China (NSFC) Grants U22A20272 and 82173807 to Y.D., NSFC grants 82225007 to

determined by assay kits. Data are presented as mean ± SD; ***$p < 0.001$ by Student's t test; $n = 8$. (E and F) Liver protein levels of ABCA1, ABCG1, ApoE, FXR, and LXRα (E) and LDLR, (p/m) SREBP2, ACC1, FASN, and SCD1 (F) were determined by western blot; $n = 4$.
(H and I) Plasma samples were collected from normal volunteers ($n = 65$) and patients with atherosclerosis ($n = 239$) to determine the levels of TC and Nogo-B, followed by comparison of TC (H) and Nogo-B (I) levels between the two groups. Data are presented as mean ± SD; ***$p < 0.001$ by Student's t test.
(J–M) Correlation between levels of Nogo-B and TC (J), LDL-C (K), HDL-C (L), and ApoE (M) in atherosclerotic patients by Pearson's correlation assay. r, correlation coefficient; p, p value by t test; $n = 239$.

H.C., and Anhui Provincial Natural Science Foundation 2308085MH240 to Y.C. We are grateful to the late Professor Jihong Han and Professor Haibo Zhu for their guidance on the study design.

AUTHOR CONTRIBUTIONS

C.X., P.Z., K.G., Q.L., Y.Y., J.L., Y.L., K.F., D.Z., and X.Y. conducted the experiments. C.X., M.W., S.C., Z.Y., T.Y., X.Z., and L.C. determined the human plasma or mice serum lipid profiles. Z.F. performed the GWAS data analysis. C.X., P.Z., S.Z., and M.Y. performed the *in vivo* studies. X.T., Y.I., L.M., and X.Z. provided the reagents and edited the paper. C.X., Y.C., H.C., and Y.D. designed the experiments and wrote the paper. Y.C., H.C., and Y.D. were responsible for the overall integration and execution of the scientific approaches.

DECLARATION OF INTERESTS

All authors declare no competing interests.

STAR★METHODS

Detailed methods are provided in the online version of this paper and include the following:

- KEY RESOURCES TABLE
- EXPERIMENTAL MODEL AND STUDY PARTICIPANT DETAILS
  - Mice
  - Human plasma collection and ELISA detection
  - Study approval
- METHOD DETAILS
  - Mendelian randomization analysis
  - Cell culture
  - *In vivo* siRNA interference
  - Plasmid construction
  - Oil red O and HE staining
  - Determination of triglyceride (TG) and total cholesterol (TC) levels
  - Determination of protein expression by immunofluorescent staining and western blot
  - Immunoprecipitation (IP)-Western blot and IP-mass spectrometry (MS) analysis
  - Quantitative RT-PCR
  - Determination of LDL binding affinity
- QUANTIFICATION AND STATISTICAL ANALYSIS

SUPPLEMENTAL INFORMATION

Supplemental information can be found online at https://doi.org/10.1016/j.celrep.2024.114691.

Received: February 14, 2024
Revised: July 9, 2024
Accepted: August 12, 2024

REFERENCES

1. Pirillo, A., Casula, M., Olmastroni, E., Norata, G.D., and Catapano, A.L. (2021). Global epidemiology of dyslipidaemias. Nat. Rev. Cardiol. *18*, 689–700. https://doi.org/10.1038/s41569-021-00541-4.
2. Andreadou, I., Iliodromitis, E.K., Lazou, A., Görbe, A., Giricz, Z., Schulz, R., and Ferdinandy, P. (2017). Effect of hypercholesterolaemia on myocardial function, ischaemia-reperfusion injury and cardioprotection by preconditioning, postconditioning and remote conditioning. Br. J. Pharmacol. *174*, 1555–1569. https://doi.org/10.1111/bph.13704.
3. Navarese, E.P., Robinson, J.G., Kowalewski, M., Kolodziejczak, M., Andreotti, F., Bliden, K., Tantry, U., Kubica, J., Raggi, P., and Gurbel, P.A. (2018). Association Between Baseline LDL-C Level and Total and Cardiovascular Mortality After LDL-C Lowering: A Systematic Review and Meta-analysis. JAMA *319*, 1566–1579. https://doi.org/10.1001/jama.2018.2525.
4. Silverman, M.G., Ference, B.A., Im, K., Wiviott, S.D., Giugliano, R.P., Grundy, S.M., Braunwald, E., and Sabatine, M.S. (2016). Association Between Lowering LDL-C and Cardiovascular Risk Reduction Among Different Therapeutic Interventions: A Systematic Review and Meta-analysis. JAMA *316*, 1289–1297. https://doi.org/10.1001/jama.2016.13985.
5. Getz, G.S., and Reardon, C.A. (2018). Apoprotein E and Reverse Cholesterol Transport. Int. J. Mol. Sci. *19*, 3479. https://doi.org/10.3390/ijms19113479.
6. Li, H., Yu, X.H., Ou, X., Ouyang, X.P., and Tang, C.K. (2021). Hepatic cholesterol transport and its role in non-alcoholic fatty liver disease and atherosclerosis. Prog. Lipid Res. *83*, 101109. https://doi.org/10.1016/j.plipres.2021.101109.
7. Luo, J., Yang, H., and Song, B.L. (2020). Mechanisms and regulation of cholesterol homeostasis. Nat. Rev. Mol. Cell Biol. *21*, 225–245. https://doi.org/10.1038/s41580-019-0190-7.
8. Ioannou, G.N. (2016). The Role of Cholesterol in the Pathogenesis of NASH. Trends Endocrinol. Metab. *27*, 84–95. https://doi.org/10.1016/j.tem.2015.11.008.
9. Wright, R.S., Ray, K.K., Raal, F.J., Kallend, D.G., Jaros, M., Koenig, W., Leiter, L.A., Landmesser, U., Schwartz, G.G., Friedman, A., et al. (2021). Pooled Patient-Level Analysis of Inclisiran Trials in Patients With Familial Hypercholesterolemia or Atherosclerosis. J. Am. Coll. Cardiol. *77*, 1182–1193. https://doi.org/10.1016/j.jacc.2020.12.058.
10. GrandPré, T., Nakamura, F., Vartanian, T., and Strittmatter, S.M. (2000). Identification of the Nogo inhibitor of axon regeneration as a Reticulon protein. Nature *403*, 439–444. https://doi.org/10.1038/35000226.
11. Acevedo, L., Yu, J., Erdjument-Bromage, H., Miao, R.Q., Kim, J.E., Fulton, D., Tempst, P., Strittmatter, S.M., and Sessa, W.C. (2004). A new role for Nogo as a regulator of vascular remodeling. Nat. Med. *10*, 382–388. https://doi.org/10.1038/nm1020.
12. Zhang, S., Guo, F., Yu, M., Yang, X., Yao, Z., Li, Q., Wei, Z., Feng, K., Zeng, P., Zhao, D., et al. (2020). Reduced Nogo expression inhibits diet-induced metabolic disorders by regulating ChREBP and insulin activity. J. Hepatol. *73*, 1482–1495. https://doi.org/10.1016/j.jhep.2020.07.034.
13. Li, J., Sun, Y., Xue, C., Yang, X., Duan, Y., Zhao, D., and Han, J. (2023). Nogo-B deficiency suppresses white adipogenesis by regulating β-catenin signaling. Life Sci. *321*, 121571. https://doi.org/10.1016/j.lfs.2023.121571.
14. Wang, X., Yang, Y., Zhao, D., Zhang, S., Chen, Y., Chen, Y., Feng, K., Li, X., Han, J., Iwakiri, Y., et al. (2022). Inhibition of high-fat diet-induced obesity via reduction of ER-resident protein Nogo occurs through multiple mechanisms. J. Biol. Chem. *298*, 101561. https://doi.org/10.1016/j.jbc.2022.101561.
15. Park, J.K., Shao, M., Kim, M.Y., Baik, S.K., Cho, M.Y., Utsumi, T., Satoh, A., Ouyang, X., Chung, C., and Iwakiri, Y. (2017). An endoplasmic reticulum protein, Nogo-B, facilitates alcoholic liver disease through regulation of kupffer cell polarization. Hepatology *65*, 1720–1734. https://doi.org/10.1002/hep.29051.
16. Lai, C.R., Tsai, Y.L., Tsai, W.C., Chen, T.M., Chang, H.H., Changchien, C.Y., Wu, S.T., Wang, H.H., Chen, Y., and Lin, Y.H. (2022). Farnesoid X Receptor Overexpression Decreases the Migration, Invasion and Angiogenesis of Human Bladder Cancers via AMPK Activation and Cholesterol Biosynthesis Inhibition. Cancers *14*, 4398. https://doi.org/10.3390/cancers14184398.
17. Defesche, J.C., Gidding, S.S., Harada-Shiba, M., Hegele, R.A., Santos, R.D., and Wierzbicki, A.S. (2017). Familial hypercholesterolaemia. Nat. Rev. Dis. Primers *3*, 17093. https://doi.org/10.1038/nrdp.2017.93.
18. Hsieh, J., Koseki, M., Molusky, M.M., Yakushiji, E., Ichi, I., Westerterp, M., Iqbal, J., Chan, R.B., Abramowicz, S., Tascau, L., et al. (2016). TTC39B

deficiency stabilizes LXR reducing both atherosclerosis and steatohepatitis. Nature *535*, 303–307. https://doi.org/10.1038/nature18628.

19. Pohl, C., and Dikic, I. (2019). Cellular quality control by the ubiquitin-proteasome system and autophagy. Science *366*, 818–822. https://doi.org/10.1126/science.aax3769.
20. Kwon, Y.T., and Ciechanover, A. (2017). The Ubiquitin Code in the Ubiquitin-Proteasome System and Autophagy. Trends Biochem. Sci. *42*, 873–886. https://doi.org/10.1016/j.tibs.2017.09.002.
21. Wang, J.Q., Li, L.L., Hu, A., Deng, G., Wei, J., Li, Y.F., Liu, Y.B., Lu, X.Y., Qiu, Z.P., Shi, X.J., et al. (2022). Inhibition of ASGR1 decreases lipid levels by promoting cholesterol excretion. Nature *608*, 413–420. https://doi.org/10.1038/s41586-022-05006-3.
22. Hiebl, V., Ladurner, A., Latkolik, S., and Dirsch, V.M. (2018). Natural products as modulators of the nuclear receptors and metabolic sensors LXR, FXR and RXR. Biotechnol. Adv. *36*, 1657–1698. https://doi.org/10.1016/j.biotechadv.2018.03.003.
23. Watanabe, M., Houten, S.M., Wang, L., Moschetta, A., Mangelsdorf, D.J., Heyman, R.A., Moore, D.D., and Auwerx, J. (2004). Bile acids lower triglyceride levels via a pathway involving FXR, SHP, and SREBP-1c. J. Clin. Invest. *113*, 1408–1418. https://doi.org/10.1172/jci21025.
24. Zhang, S., Yu, M., Guo, F., Yang, X., Chen, Y., Ma, C., Li, Q., Wei, Z., Li, X., Wang, H., et al. (2020). Rosiglitazone alleviates intrahepatic cholestasis induced by α-naphthylisothiocyanate in mice: The role of circulating 15-deoxy-Δ(12,14) -PGJ(2) and Nogo. Br. J. Pharmacol. *177*, 1041–1060. https://doi.org/10.1111/bph.14886.
25. Song, Y., Liu, J., Zhao, K., Gao, L., and Zhao, J. (2021). Cholesterol-induced toxicity: An integrated view of the role of cholesterol in multiple diseases. Cell Metab. *33*, 1911–1925. https://doi.org/10.1016/j.cmet.2021.09.001.
26. Hu, W., Zhang, W., Chen, Y., Rana, U., Teng, R.J., Duan, Y., Liu, Z., Zhao, B., Foeckler, J., Weiler, H., et al. (2016). Nogo-B receptor deficiency increases liver X receptor alpha nuclear translocation and hepatic lipogenesis through an adenosine monophosphate-activated protein kinase alpha-dependent pathway. Hepatology *64*, 1559–1576. https://doi.org/10.1002/hep.28747.
27. Tian, L., Song, Y., Xing, M., Zhang, W., Ning, G., Li, X., Yu, C., Qin, C., Liu, J., Tian, X., et al. (2010). A novel role for thyroid-stimulating hormone: up-regulation of hepatic 3-hydroxy-3-methyl-glutaryl-coenzyme A reductase expression through the cyclic adenosine monophosphate/protein kinase A/cyclic adenosine monophosphate-responsive element binding protein pathway. Hepatology *52*, 1401–1409. https://doi.org/10.1002/hep.23800.
28. Seok, S., Fu, T., Choi, S.E., Li, Y., Zhu, R., Kumar, S., Sun, X., Yoon, G., Kang, Y., Zhong, W., et al. (2014). Transcriptional regulation of autophagy by an FXR-CREB axis. Nature *516*, 108–111. https://doi.org/10.1038/nature13949.
29. Sato, R., Goldstein, J.L., and Brown, M.S. (1993). Replacement of serine-871 of hamster 3-hydroxy-3-methylglutaryl-CoA reductase prevents phosphorylation by AMP-activated kinase and blocks inhibition of sterol synthesis induced by ATP depletion. Proc. Natl. Acad. Sci. USA *90*, 9261–9265. https://doi.org/10.1073/pnas.90.20.9261.
30. Clarke, P.R., and Hardie, D.G. (1990). Regulation of HMG-CoA reductase: identification of the site phosphorylated by the AMP-activated protein kinase in vitro and in intact rat liver. EMBO J *9*, 2439–2446. https://doi.org/10.1002/j.1460-2075.1990.tb07420.x.
31. Wellington, C.L., Brunham, L.R., Zhou, S., Singaraja, R.R., Visscher, H., Gelfer, A., Ross, C., James, E., Liu, G., Huber, M.T., et al. (2003). Alterations of plasma lipids in mice via adenoviral-mediated hepatic overexpression of human ABCA1. J. Lipid Res. *44*, 1470–1480. https://doi.org/10.1194/jlr.M300110-JLR200.
32. Basso, F., Freeman, L., Knapper, C.L., Remaley, A., Stonik, J., Neufeld, E.B., Tansey, T., Amar, M.J.A., Fruchart-Najib, J., Duverger, N., et al. (2003). Role of the hepatic ABCA1 transporter in modulating intrahepatic cholesterol and plasma HDL cholesterol concentrations. J. Lipid Res. *44*, 296–302. https://doi.org/10.1194/jlr.M200414-JLR200.
33. Vrins, C., Vink, E., Vandenberghe, K.E., Frijters, R., Seppen, J., and Groen, A.K. (2007). The sterol transporting heterodimer ABCG5/ABCG8 requires bile salts to mediate cholesterol efflux. FEBS Lett. *581*, 4616–4620. https://doi.org/10.1016/j.febslet.2007.08.052.
34. Mudaliar, S., Henry, R.R., Sanyal, A.J., Morrow, L., Marschall, H.U., Kipnes, M., Adorini, L., Sciacca, C.I., Clopton, P., Castelloe, E., et al. (2013). Efficacy and safety of the farnesoid X receptor agonist obeticholic acid in patients with type 2 diabetes and nonalcoholic fatty liver disease. Gastroenterology *145*, 574–582.e1. https://doi.org/10.1053/j.gastro.2013.05.042.
35. Neuschwander-Tetri, B.A., Loomba, R., Sanyal, A.J., Lavine, J.E., Van Natta, M.L., Abdelmalek, M.F., Chalasani, N., Dasarathy, S., Diehl, A.M., Hameed, B., et al. (2015). Farnesoid X nuclear receptor ligand obeticholic acid for non-cirrhotic, non-alcoholic steatohepatitis (FLINT): a multicentre, randomised, placebo-controlled trial. Lancet *385*, 956–965. https://doi.org/10.1016/s0140-6736(14)61933-4.
36. Duan, Y., Zhang, F., Yuan, W., Wei, Y., Wei, M., Zhou, Y., Yang, Y., Chang, Y., and Wu, X. (2019). Hepatic cholesterol accumulation ascribed to the activation of ileum Fxr-Fgf15 pathway inhibiting hepatic Cyp7a1 in high-fat diet-induced obesity rats. Life Sci. *232*, 116638. https://doi.org/10.1016/j.lfs.2019.116638.
37. Kong, B., Wang, L., Chiang, J.Y.L., Zhang, Y., Klaassen, C.D., and Guo, G.L. (2012). Mechanism of tissue-specific farnesoid X receptor in suppressing the expression of genes in bile-acid synthesis in mice. Hepatology *56*, 1034–1043. https://doi.org/10.1002/hep.25740.
38. Fessler, M.B. (2018). The challenges and promise of targeting the Liver X Receptors for treatment of inflammatory disease. Pharmacol. Ther. *181*, 1–12. https://doi.org/10.1016/j.pharmthera.2017.07.010.
39. Rice, A.S.C., Morland, R., Huang, W., Currie, G.L., Sena, E.S., and Macleod, M.R. (2013). Transparency in the reporting of in vivo pre-clinical pain research: The relevance and implications of the ARRIVE (Animal Research: Reporting In Vivo Experiments) guidelines. Scand. J. Pain *4*, 58–62. https://doi.org/10.1016/j.sjpain.2013.02.002.
40. Liu, S., Yang, K., Zhang, H., Yang, Q., and Bai, Y. (2023). The bidirectional causal association between psoriasis and psychological illnesses: a 2-sample Mendelian randomization study. Arch. Dermatol. Res. *316*, 40. https://doi.org/10.1007/s00403-023-02736-w.
41. Chen, X., Hong, X., Gao, W., Luo, S., Cai, J., Liu, G., and Huang, Y. (2022). Causal relationship between physical activity, leisure sedentary behaviors and COVID-19 risk: a Mendelian randomization study. J. Transl. Med. *20*, 216. https://doi.org/10.1186/s12967-022-03407-6.
42. Lein, A., Baumgartner, W.D., Riss, D., Gstöttner, W., Landegger, L.D., Liu, D.T., Thurner, T., Vyskocil, E., and Brkic, F.F. (2024). Early Results With the New Active Bone-Conduction Hearing Implant: A Systematic Review and Meta-Analysis. Otolaryngol. Head Neck Surg. *170*, 1630–1647. https://doi.org/10.1002/ohn.728.
43. Daugherty, A., Tall, A.R., Daemen, M.J.A.P., Falk, E., Fisher, E.A., García-Cardeña, G., Lusis, A.J., Owens, A.P., American Heart Association Council on Arteriosclerosis, Thrombosis and Vascular Biology; and Council on Basic Cardiovascular Sciences; Rosenfeld, M.E., and Virmani, R. (2017). Recommendation on Design, Execution, and Reporting of Animal Atherosclerosis Studies: A Scientific Statement From the American Heart Association. Circ. Res. *121*, e53–e79. https://doi.org/10.1161/res.0000000000000169.

STAR★METHODS

KEY RESOURCES TABLE

REAGENT or RESOURCE	SOURCE	IDENTIFIER
Antibodies		
α-tubulin (1:1000)	UTIBODY, China	Cat# UM4007
ABCA1 (1:1000)	Novus Biologicals, USA	NB400-105 RRID:AB_10000630
ABCG1 (1:1000)	Proteintech Group, USA	13578-1-AP RRID:AB_2220174
ABCG5 (1:1000)	Proteintech Group, USA	27722-1-AP RRID:AB_2880952
ABCG8 (1:1000)	Novus Biologicals, USA	NBP1-71706 RRID:AB_11022553
ACC1 (1:1000)	ABclonal, China	A15606 RRID:AB_2763012
ApoE (1:1000)	Santa Cruz Biotechnology, USA	sc-98574 RRID:AB_2058119
HRP-conjugated β-actin (1:3000)	ABclonal, China	AC028 RRID:AB_2769861
BRCA1 (1:1000)	ABclonal, China	A11034 RRID:AB_2758380
BARD1 (1:1000)	ABclonal, China	A1685 RRID:AB_2763738
FASN (1:1000)	Santa Cruz Biotechnology, USA	sc-55580 RRID:AB_2231427
Flag (1:2000)	Abmart, China	M2008
FXR (1:1000)	Novus Biologicals, USA	NBP2-16550
HRP-conjugated GAPDH (1:10000)	Proteintech Group, USA	HRP-60004 RRID:AB_2737588
GFP (1:2000)	Proteintech Group, USA	50430-2-AP RRID:AB_11042881
Lamin A/C	Proteintech Group, USA	10298-1-AP RRID:AB_2296961
LDLR (1:1000)	Proteintech Group, USA	10785-1-AP RRID:AB_2281164
LXRα (1:1000)	Proteintech Group, USA	14351-1-AP RRID:AB_10640525
Nogo-B (1:1000)	Novus Biologicals, USA	NB100-56681 RRID:AB_838641
SCD1 (1:1000)	Santa Cruz Biotechnology, USA	sc-515844
SREBP1 (1:500)	Novus Biologicals, USA	NB100-2215 RRID:AB_10002406
SREBP2 (1:500)	Proteintech Group, USA	28212-1-AP RRID:AB_2881091
Ubiquitin (1:1000)	Proteintech Group, USA	10201-2-AP RRID:AB_671515
Biological samples		
Plasma samples from volunteers and patients with coronary atherosclerosis	The First Affiliated Hospital of University of Science and Technology of China	Ethics acceptance number: 2022-ky303
Chemicals, peptides, and recombinant proteins		
High-cholesterol diet	Research diets (New jersey, USA)	D12109C
Oil red O	Sigma-Aldrich (St. Louis, USA)	O0625
iScript cDNA Synthesis Kit	Bio-Rad Laboratories, Inc. (Hercules, USA)	1708890
SYBR Green PCR Master Mix	Vazyme Biotech Co. (Nanjing, China)	Q111-02
Control siRNA (*in vitro*)	Riobobio Co. (Suzhou, China)	siN0000001
Nogo-B siRNA (*in vitro*)	Riobobio Co. (Suzhou, China)	siB160409124904
FXR siRNA (*in vitro*)	Riobobio Co. (Suzhou, China)	siBDM0001
Human DiI-LDL	Yeasen (Shanghai, China)	20614ES76
Cycloheximide	Sigma-Aldrich (Louis, USA)	C7698
MG132	MedChemExpress (Shanghai, China)	HY-13259
3-Methyladenine	MedChemExpress (Shanghai, China)	HY-19312
ClonExpress II One Step Cloning Kit	Vazyme Biotech Co. (Nanjing, China)	C112-01
Hieff Trans™ Liposomal Transfection Reagent	Yeasen Biotechnology Co., Ltd. (Shanghai, China)	40802ES03
Entranster™-in vivo	Engreen Biosystem, Ltd. (Beijing, China)	18668-11-1
Anti-GFP magnetic bead	Biolinkedin (Shanghai, China)	L-1016
rProtein G MagPoly beads	ABclonal (Wuhan, China)	RM02843
T0901317	Cayman Chemical (Michigan, USA)	71810

(*Continued on next page*)

Continued

REAGENT or RESOURCE	SOURCE	IDENTIFIER
Critical commercial assays		
Human RTN4 (Nogo) ELISA kit	CUSABIO Biotech Co. (Wuhan, China)	CSB-EL020572HU
Human ApoE ELISA kit	Ruixin Biotech Co. (Quanzhou, China)	RX104841H
Mouse Nogo-B ELISA kit	Ruixin Biotech Co. (Quanzhou, China)	RX104302M
Nuclear protein extraction kit	Solarbio Science & Technology Co., Ltd. (Beijing, China)	R0050
Human Lp(a) ELISA kit	Cloud-Clone Corp Co. (Wuhan, China)	SEA842Hu
Human ApoB ELISA kit	Ruixin Biotech Co. (Quanzhou, China)	
Tissue cholesterol content assay	Solarbio Science & Technology Co., Ltd. (Beijing, China)	BC1985
Tissue triglyceride content assay	Solarbio Science & Technology Co., Ltd. (Beijing, China)	BC0625
Total bile acid microplate assay kit	COHESION BIOSCIENCES (London, UK)	CAK1166
Experimental models: Cell lines		
293t	ATCC	Cat# CRL-3216
HepG2	ATCC	Cat# HB-8065
Experimental models: Organisms/strains		
Mouse: C57BL/6JGpt	GemPharmatech (Nanjing, China)	N/A
Mouse: C57BL/6JGpt-Nogo^{em27Cd30269}/Gpt	GemPharmatech (Nanjing, China)	N/A
Mouse: C57BL/6JGpt-ApoE^{em1Cd82}/Gpt	GemPharmatech (Nanjing, China)	N/A
Mouse: C57BL/6JGpt-LDLR^{em1Cd82}/Gpt	GemPharmatech (Nanjing, China)	N/A
Oligonucleotides		
See Table S1	This paper	N/A
Control siRNA (*in vitro*)	Riobobio Co. (Suzhou, China)	siN0000001
Nogo-B siRNA (*in vitro*)	Riobobio Co. (Suzhou, China)	siB160409124904
FXR siRNA (*in vitro*)	Riobobio Co. (Suzhou, China)	siBDM0001
Control siRNA (*in vivo*)	GENEWIZ (Suzhou, China)	N/A
Nogo-B siRNA (*in vivo*)	GENEWIZ (Suzhou, China)	N/A
Recombinant DNA		
pEGFP-C2-Nogo-B (human)	This paper	N/A
pEGFP-C2-LXRα (mouse)	This paper	N/A
pcDNA-LXRα-Flag (human)	This paper	N/A
pcDNA3.1-Nogo-B (mouse)	This paper	N/A
AAV8-TBG-EGFP-miR30-shControl	ViGene Biosciences, (Shandong, China)	N/A
AAV8-TBG-EGFP-miR30-shNogo-B	ViGene Biosciences, (Shandong, China)	N/A
Software and algorithms		
GraphPad Prism 9.5	GraphPad	https://www.graphpad.com/
ImageJ	ImageJ	https://imagej.nih.gov/ij/
Adobe Photoshop CS6	Adobe	https://www.adobe.com
R Bioconductor project package limma	The R Foundation	https://www.r-project.org/
R package ggplot2	The R Foundation	https://www.r-project.org/

EXPERIMENTAL MODEL AND STUDY PARTICIPANT DETAILS

Mice

LDLR deficient (LDLR$^{-/-}$) and ApoE deficient (ApoE$^{-/-}$) mice with C57BL/6J background were purchased from GemPharmatech Co., Ltd. (Nanjing, China). ApoE$^{-/-}$LDLR$^{-/-}$ double deficient mice were generated by crossing ApoE$^{-/-}$ with LDLR$^{-/-}$ mice. ApoE$^{+/-}$ and LDLR$^{+/-}$ dual heterozygous (ApoE$^{+/-}$LDLR$^{+/-}$) mice were produced by mating male LDLR$^{-/-}$ApoE$^{-/-}$ mice with female C57BL/6J mice. Nogo deficient (Nogo$^{-/-}$) mice with C57BL/6J background were obtained from GemPharmatech Co., Ltd. (Nanjing, China). Nogo and ApoE or Nogo and LDLR double deficient (ApoE$^{-/-}$Nogo$^{-/-}$ or LDLR$^{-/-}$Nogo$^{-/-}$) mice were generated by crossing Nogo$^{-/-}$ mice with ApoE$^{-/-}$ or LDLR$^{-/-}$ mice. All mice were housed in SPF units in the Animal Center of the College of Life Sciences, Nankai University (Tianjin, China) at 20 ± 2°C with a relative humidity of 60–70% and 12 h light/dark cycles. All the animals had free

access to water and normal chow, and HCD contains 20% fat, 1.25% cholesterol and 0.5% sodium cholate during the treatment. The mice were kept in standard cages (≤5 mice per cage). Mice were allowed to acclimatize to the housing environment for at least 7 days before experiments. All the treatments were conducted in a blinded fashion. During the treatment, animals were checked food intake, water drinking and bodyweight routinely.

To investigate the effect of Nogo-B deficiency on hypercholesterolemia, the Nogo$^{+/+}$, Nogo$^{-/-}$ (8-week-old, males), ApoE$^{-/-}$ and ApoE$^{-/-}$Nogo$^{-/-}$ (8-week-old, males), LDLR$^{-/-}$, LDLR$^{-/-}$Nogo$^{-/-}$ (8-week-old, males), ApoE$^{+/-}$LDLR$^{+/-}$ mice (6-week-old, males) injected si-Ctrl or si-Nogo-B, and wild-type C57BL/6JGpt mice (8-week-old, males) injected with AAV8-TBG-shControl or AAV-TBG-shNogo-B were fed HCD containing 20% fat, 1.25% cholesterol and 0.5% sodium cholate for 3, 16, 16, 26, and 5 weeks, respectively. At the end of treatment, all the mice were anesthetized with isoflurane (2% isoflurane/0.2 L O_2/min), followed by collection of blood samples. Mice were then euthanized for collection of aorta, liver, and other tissue samples individually. Serum was prepared to determine levels of TC, HDL-C, LDL-C, TG, and activity of AST, ALP or ALT. Serum Nogo-B levels were determined by ELISA using the commercially available kits purchased from Ruixin Biotech Co (Quanzhou, China).

Male Nogo$^{+/+}$ and Nogo$^{-/-}$ mice (6-week-old) were randomly divided into 2 groups (n = 6), respectively. Normal chow-fed mice were treated with T0901317 (T317 group) at 1 mg/kg bodyweight/day dissolved in the mixture of DMSO and corn oil (1:9) or vehicle (vehicle group, the mixture of DMSO and corn oil) by oral gavage for 9 d. Mice were i.p. injected with 3 mL thioglycollate solution at the 5th day of treatment. At the end of treatment (9 days after 1st T317 treatment), mouse serum and liver samples were collected.

To knock down hepatic Nogo-B expression, AAV8-TBG-EGFP-miR30-shNogo-B (AAV-Nogo-B) vector was constructed (ViGene Biosciences, Shandong, China), and AAV8-TBG-EGFP-miR30-shRNA vector inserted with scramble sequence (AAV8-shControl) was used as a control. 8-week-old male wildtype C57BL/6J mice were randomly divided into 2 groups (n = 8), and intravenously injected with AAV8-shNogo-B and AAV8-shControl separately. Mice were fed with HCD for 5 weeks. After fasting overnight, mice were euthanized and serum, bile, liver, and fecal were collected.

Human plasma collection and ELISA detection

Based on the results of coronary angiography and intravascular ultrasound evaluation, the subjects were divided into normal volunteers (with no known history of coronary heart disease or renal disease and no severe coronary stenosis observed by coronary angiography either) and atherosclerosis group (the 2018 JCS Guide "Diagnosis and Treatment of Acute Coronary Syndrome" as the diagnostic criteria). Age and sex were matched between normal volunteers and patients with atherosclerosis with random sampling.

The exclusion criteria: blood tests for liver function, urea nitrogen, creatinine and uric acid to exclude any cases of combined liver or renal dysfunction; patients with severe heart failure, acute stroke, refractory hypertension, acute and chronic infection, blood system diseases, severe bleeding, autoimmune diseases, malignant tumors, severe trauma or non-atherosclerosis caused by acute myocardial infarction; patients who regularly take anti-myocardial ischemia drugs for more than 1 week before the onset; those who have a history of old myocardial infarction. All samples were collected before patients received systemic anti-myocardial ischemia drugs and revascularization therapy.

Human blood samples were collected through the median cubital vein from the all individuals with informed consent. After standing, the blood samples were centrifuged for 20 min at 2,000 g. The plasma was then collected and stored in a −80°C freezer for assay. Although the ELISA kit may react with other members of Nogo family, based on our studies, Nogo-B is the only member detectable in the blood by Western blot. Therefore, we still used the term of "Nogo-B" for plasma samples in this study. Levels of Nogo-B, ApoB, ApoE, Lp(a), TG, TC, LDL-C, and HDL-C in human plasma were determined either by an automated biochemical analyzer (model 3100; Hitachi High-Technologies Corporation, Tokyo, Japan) or by the correspondingly assay kits based on the manufacturer's instruction.

Study approval

The protocols for *in vivo* study with mice were approved by the Ethics Committee of Nankai University (2022-SYDWLL-000574) and conformed to the Guide for the Care and Use of Laboratory Animals published by National Institutes of Health (NIH). The animal studies were reported in compliance with the ARRIVE guidelines.[39]

All studies with human blood samples were approved by the regional Ethical Committees and adhered strictly to the Declaration of Helsinki Principle 2008. All the subjects enrolled in this study were hospitalized in the First Affiliated Hospital of the University of Science and Technology of China (ethics acceptance number: 2022-ky303) and clinically diagnosed by coronary angiography with complete medical records, clinical parameters and follow-up data.

METHOD DETAILS

Mendelian randomization analysis

This study uses a two-sample Mendelian randomization analysis to examine the relationship between Nogo and cholesterol levels. The general process is as follows: cohort information was obtained from the GWAS database (ID number: ebi-a-GCST90013882). First, single-nucleotide polymorphisms (SNPs) strongly associated with the exposure factors were selected as instrumental variables, with linkage disequilibrium SNPs and weak instrumental variables removed.[40] Data were analyzed using the inverse variance

weighted method,[41] and causal relationships were assessed using a fixed-effects model.[42] All statistical tests were two-sided, and data analysis was conducted using the R package "TwoSampleMR" (version 0.5.6).

Cell culture

All the cell lines were purchased from ATCC (Manassas, USA). HepG2 cells were cultured in MEM medium containing 10% FBS, 50 μg/mL penicillin/streptomycin and 2 mmol/L glutamine. HepG2 cells with Nogo-B deficiency (named as Cas9-Nogo-B cells) and the corresponding control cells (named as Cas9-Ctrl cells) were generated by CRISPR-Cas9. The sgRNA sequences of Nogo-B were 5′-CGTTCAAGTACCAGTTCGTG-3′, which locates in the first exon 63 bp downstream of the start codon.[24] siRNA used for *in vitro* experiments was purchased from Riobobio (Guangzhou, China).

In vivo siRNA interference

The 6-week-old male ApoE$^{+/-}$LDLR$^{+/-}$ mice were pre-fed mHFD for 20 w, then divided into 2 groups randomly (n = 10/group) and intravenously (i.v.) injected control scramble siRNA (si-Ctrl) (n = 10) and siRNA against Nogo-B (si-Nogo-B) (n = 10) from tail vein, using the Entranster-*in vivo* transfection reagent purchased from Engreen Biosystem Co., Ltd. (Beijing, China) according to the manufacturer's instructions. Both control siRNA and Nogo-B siRNA were synthesized by GENEWIZ (Suzhou, China). The sequences for si-Ctrl are 5′-UUCUCCGAACGUGUCACGUdTdT-3' (sense) and 5′-ACGUGACACGUUCGGAGAAdTdT-3' (antisense). The sequences for si-Nogo-B are mixed from 3 pairs of different targets which were named as si-Nogo-B #1, #2, #3. si-Nogo-B #1: 5′-GGAUCUCAUUGUAGUCAUATT-3' (sense) and 5′-UAUGACUACAAUGAGAUCCTT-3' (antisense); si-Nogo-B #2: 5′-GCAGU GUUGAUGUGGGUAUUUTT-3' (sense) and 5′-AAAUACCCACAUCAACACUGCTT-3' (antisense); si-Nogo-B #3: 5′-CACAUAAA CUAGGAAGAGATT-3' (sense) and 5′-UCUCUUCCUAGUUUAUGUGTT-3' (antisense). Mice were i.v. injected siRNA mixed with transfection reagent once a week for the first 5 w and twice for the last week. At the end of experiment (three days after the last siRNA injection), mice were euthanized, followed by collection of tissue samples.

Plasmid construction

Nogo-B and LXRα expression vectors were constructed as follows. Human and mouse complementary DNA (cDNA) was synthesized with RNA extracted from HepG2 cells and mouse liver tissue, respectively. The plasmids were constructed using the cDNA and primers with the sequences listed in Table S4 and the ClonExpress II One Step Cloning Kit (Vazyme, Nanjing, China).

Oil red O and HE staining

Aortas were collected and separated carefully from other tissues. After fixed in 4% paraformaldehyde for 24 h, aortas were washed with PBS for 3 times and then stained with oil red O solution. Each entire aorta was dissected to assess *en face* lesions except aortic root which was used to prepare frozen cross section for determination of sinus lesions. Atherosclerotic lesions in *en face* aorta and sinus lesions in cross section of aortic root were calculated by 2 individuals who were blinded to the experimental design and each other's results using a computer-assisted image analysis protocol, according to the guidelines for experimental atherosclerosis studies described in the American Heart Association statement.[43] Lesions are expressed as mean percentage of lesion areas in the aorta or as μm^2 per section plus standard deviation (SD). Oil red O positive staining areas in aortic root cross sections were also determined and expressed as μm^2 per section. The frozen liver sections prepared from the vehicle or T317-treated mice and 3-week HCD-fed mice were conducted oil red O staining for determination of lipid content in the liver.

Thickness of fibrotic caps and necrotic core areas in lesion areas were determined after HE staining. All images were captured with a Leica DM5000B microscope (Wetzlar, Germany).

Determination of triglyceride (TG) and total cholesterol (TC) levels

To determine liver TG or TC content, ~100 mg liver/feces was weighed and ground in the tissue lysis buffer, based on the instructions for triglyceride Labassay kit (Wako Chemical, Osaka, Japan) and tissue cholesterol content assay kit (Applygen Technologies Inc., Beijing, China). 10 μL bile were directly used to detect total cholesterol levels as the instructions of the assay kit. Liver TC and TG content was finally normalized by tissue protein content.

Determination of protein expression by immunofluorescent staining and western blot

Expression of Nogo-B and LXRα in Cas-9 Ctrl and Cas9-Nogo-B HepG2 cells was determined by immunofluorescent staining with the corresponding primary antibody and captured by fluorescence confocal microscope. Expression of the target protein was determined by Western blot with total or nuclear proteins.[24]

Immunoprecipitation (IP)-Western blot and IP-mass spectrometry (MS) analysis

Mouse pcDNA3.1-Nogo-B, pEGFP-C2-LXRα plasmids and human pEGFP-C2-Nogo-B, pcDNA3-LXRα-Flag plasmids were used to transfect 293T cells simultaneously using Hieff Trans Liposomal Transfection Reagent (YEASEN, Shanghai, China) for 48 h, respectively (empty plasmid without inserted DNA fragment for control). Cells were lysed and incubated with anti-GFP magnetic bead based on the manufacturer's instruction (Biolinkedin, Shanghai, China). Beads were washed 3 times and boiled in a metal bath. Supernatants were separated by SDS-PAGE and analyzed by Western blot using anti-GFP and anti-Nogo antibodies.

Human LXRα-Flag plasmid was used to transfect Cas9-Ctrl and Cas9-Nogo-B HepG2 cells as indicated for 48 h. Cells were then treated with 10 μM MG132 for 2 h, followed by preparation of total protein extract. The same amount of total protein extract from each sample was added with anti-Flag antibody and incubated at room temperature for 1 h, followed by addition of rProtein G MagPoly beads (ABcloanl, Wuhan, China) and incubation for 30 min based on the manufacturer's instruction. The subsequent immunoblotting was conducted with anti-ubiquitin, LXRα or Flag antibody.

Briefly, HepG2 cells transfected with pEGFP-C2-Nogo-B were split by cell lysate and protein extraction was incubated with anti-GFP antibody and rProtein G MagPoly beads as manufacturer's instruction. The sample was then subjected to SDS-PAGE assay. The part of gel was collected for MS assay by Novogene Bioinformatics Technology Co., Ltd (Beijing, China).

Quantitative RT-PCR

After treatment, RNA was extracted from tissues or cells using Trizol reagent (Invitrogen) according to the manufacturer's instructions. cDNA was synthesized using iScript cDNA Synthesis Kit (Bio-Rad, Hercules, USA). Individual quantitative PCR (qPCR) was performed using SYBR Green PCR Master Mix (Vazyme, Nanjing, China) and the primers with sequences listed in Table S1 mRNA levels were normalized by levels of glyceraldehyde-3-phosphate dehydrogenase (GAPDH) mRNA in the corresponding samples.

Determination of LDL binding affinity

Cas9-Nogo-B and Cas9-Ctrl HepG2 cells or 24 h-Ctrl siRNA and Nogo-B siRNA transfected HepG2 cells were cultured in medium containing 20 μg/mL human DiI-LDL solution [human LDL labeled with fluorescence probe DiI (1,1′-dioctadecyl-3,3,3′,3′-tetramethylindocarbocyanine perchlorate)] for 4 h. Cells were then washed with fresh medium for 3 times. After fixed in 4% paraformaldehyde for 30 min, cells were stained with a DAPI solution to detect the nucleus. Images of the sections were obtained with a fluorescence microscope (Leica DM5000B).

QUANTIFICATION AND STATISTICAL ANALYSIS

After capture, the intensity of each image was quantified by who was blinded to the treatment with segmentation color-threshold analysis using Photoshop software. All data were generated from at least three independent experiments. Each value was presented as the mean ± SD. The raw data were initially conducted the analysis of normal distribution using Shapiro-Wilk method followed by Levene test for the homogeneity of the variances. For animal and cellular experiments, a two-tailed unpaired student's t-test was performed to compare two groups. One-way or two-way ANOVA was used to compare more than two groups. The correlation between human plasma Nogo-B and ApoE, TG, TC, LDL-C, and HDL-C was estimated by Pearson's method.

Information on technical and/or biological replicates and statistical tests for each experiment can be found in the figure legends.